UNIVERSITI MALAYSIA PAHANG

Faculty of Chemical Engineering Technology and Process

FINAL REPORT

RDU 170322

DEVELOPMENT OF GLUTAMIC ACID INCORPORATED WITH FLUORINE IONIC LIQUID FOR DISSOLUTION OF SOLID SCALE

PROF. MADYA DR. FATMAWATI BINTI ADAM

UMP

ABSTRACT

Solid scale formation such as calcite ($CaCO_3$), barite ($BaSO_4$) and ferrite (FeS) in oil production is known to be one of the major problems that cost operator huge amount of expenditure. Chemical compound with carboxylic group and amine has been widely used due to its ability to dissolve and chelate metal ions in solid scale to prevent reprecipitation. This research aims to to synthesise and characterise the amino acid-based solid scale dissolver from monosodium glutamate (MSG). The second objective is to evaluate the dissolution of calcite and barite solid scale using synthesised amino acid-based solid scale dissolver. Acidification produces two amino based dissolver, glutamic acid hydrochloride (solid) and glutamic acid hydro fluoroborate (liquid). Metathesis produces glutamic acid trifluoromethyl sulfonate (liquid). Glutamic acid hydrochloride can dissolve 3865 ppm of calcium in 24 hours at 60 °C and less than 5ppm of barium. Glu-BF_4 can dissolve up to 2381 ppm of calcium and only 74 ppm of barium. GluTFMS can dissolve up to 2013.5 ppm of calcium and 60.0 ppm of barite. Based on the dissolution result, GluCl, GluBF4 and Glu TFMS is a good dissolver for calcite as it can dissolve more than 2000 ppm of calcite at low concentration. Barite is known as the most difficult solid scale to dissolve. In this study, all dissolver synthesised can only dissolve less than 100 ppm of barite.

ABSTRAK

Pembentukan kerak pepejal dalam pengeluaran minyak dan gas dikenal pasti sebagai salah satu masalah utama yang memerlukan perbelanjaan besar pengendalian telaga minyak. Kerja intervensi yang paling biasa dilakukan bagi menyelesaikan masalah kerak pepejal adalah rawatan kimia untuk melarutkan atau merencat pembentukan kerak pepejal. Antara skala pepejal yang ada dalam pengeluaran minyak adalah kalsit ($CaCO_3$) dan barit ($BaSO_4$). Kalsit adalah salah satu masalah skala pepejal yang paling biasa dalam pengeluaran minyak terjadi hasil dari kehilangan tekanan. Kehadiran skala pepejal barit disebabkan peningkatan suhu dan kandungan garam yang tinggi. Ia adalah kerak pepejal paling tidak larut dan sangat sukar untuk dihapuskan. Asid sering digunakan untuk melarutkan kerak pepejal, walau bagaimanapun, ia boleh menyebabkan masalah kakisan yang teruk. Bahan kimia dengan kumpulan karboksilik dan amina telah digunakan secara meluas kerana keupayaannya untuk melarutkan dan menghancurkan ion logam dalam kerak pepejal dan mengelakkan pemendakan semula. Objektif kajian ini adalah untuk mensintesis dan mencirikan pelarut berasaskan asid amino dari mononatrium glutamat (MSG). Objektif kedua adalah untuk menilai pelarutan kerak pepejal kalsit dan barit dengan menggunakan pelarut berasaskan asid amino yang disintesis. Pengasidan menghasilkan dua pelarut berasaskan amino, asid glutamt hidroklorik (pepejal) dan asid glutamat hidro floroborik (cecair). Metatesis menghasilkan asid glutamat trimethysulfonat (pepejal). Hydrochloride asid glutamat boleh melarutkan 3865 ppm kalsium dalam 24 jam pada 60 ° C dan kurang daripada 5ppm barium. Glu-BF_4 boleh melarutkan sehingga 2381 ppm kalsium dan hanya 74 ppm barium. GluTFMS boleh melarutkan hingga 2013.5 ppm kalsium dan 60.0 ppm barit. Berdasarkan hasil pembubaran, GluCl, GluBF_4 dan Glu TFMS adalah pelarut yang baik untuk kalsit kerana dapat melarutkan lebih dari 2000 ppm calcite pada kepekatan rendah. Barit dikenali sebagai kerak pepejal yang paling sukar untuk dilarutkan. Dalam kajian ini, ketiga-tiga dissolver disintesis hanya boleh melarutkan kurang daripada 100 ppm barit.

TABLE OF CONTENT

CHAPTER 1

INTRODUCTION

1.1 Research Background

In oil upstream production, well stimulation has become one of the important parts in the well intervention. Well flow may be reduced or stopped due to several factors including a reduction in the well pressure, blocking of reservoir pore near the drainage area and scale formation in a wellbore that blocks the flow of the fluid (Ghalambor & Economides, 2002). This problem often contributed by solid deposition comes from the inside of the reservoir itself (Crabtree et al., 1999). Well completion involved pumping of high-pressure drilling fluid into the wellbore that probably damages the surrounding formation in the reservoir. This damage will introduce solid particle such as sand and clay into the reservoir pores and reduce the oil flow towards the drainage area or block the drainage area itself (Economides, 2012). The solid scale might also come from the precipitation of solids from produced water inside the well containing dissolved solids such as calcium, barium and iron (Ghalambor & Economides, 2002; Merdhah & Yassin, 2007; Muryanto et al., 2014; Nasr-El-Din & Al-Humaidan, 2001). In addition, completion might involve the injection of brine into the well formation to maintain reservoir pressure and sweep the oil to the production well. This injection may result in co-mingling of the dissolved salt in the produced water with the additional dissolve solid in a brine solution, potentially increase precipitation solid in well tubular (Crabtree et al., 1999; Houseworth, 2013).

The deposited material forming scale has been considered as one of a major problem in oil and gas production (Dunn & Yen, 1999). One of the recorded scale problems was in the North Sea, Miller field where scale causes the production fall from 4770 m^3/d to zero in just 24 hours (Brown, 1998). To improve the reservoir flow,

stimulation method such as acid treatment often used. This method will dissolve the solid scale such as calcite and recover the permeability of the well formation (Smith & Hendrickson, 1965). Acid stimulation or commonly known as matrix acidizing is a classic well stimulation technique. First introduced in the 1930s, the treatment was done on limestone and dolomitic reservoirs formation. Acid was pumped to dissolve rock resulting in enlarging the flow towards the drainage area. Acid also used to dissolve carbonate scale or drilling mud that block the flow channels (Di Lullo & Rae, 1996). For sandstone reservoir, hydrofluoric acid mixed with hydrochloric acid commonly used and hydrochloric acid or acetic acid for limestone and carbonate formation (Rajeev et al., 2012).

With the advancement of chemical synthesis and understanding of solid scale properties, the new solvent agent called chelating agent has been introduced to reduce the usage of acid in well intervention and stimulation. The chelating agent is a solvent used to chelate metal ions and control the undesirable metal ions reaction by forming multiple bonds with the metal ion. This makes it suitable to be applied for formation clean-up and stimulating well through addition into stimulation acid to avoid precipitation of metals ions(Wayne W. Frenier et al., 2000; Portier et al., 2009). However, chelating agent is selective on the heavy metals it can chelate (Dunn & Yen, 1999; W. W. Frenier et al., 2013; Lepage et al., 2011) and may have a bad impact on the environment by increasing the toxicity of heavy metals (iron) compare to its respective free ions (Sillanpaa & Oikari, 1996) as well as improving the heavy metal mobilisation and bioavailability in environment (Means et al., 1978). Nevertheless, the chelating agent can be regarded as the best replacement for non-acidic chemicals stimulation for solid scale control.

Other than nitrogen, chelating agents used in control of calcite and barite commonly contains a notable number of the carboxylic group that will act as a ligand in chelating the metal ions (Bageri et al., 2017; Lepage et al., 2011; M. A. Mahmoud et al., 2011; Moghadasi et al., 2007) All amino acid contains both nitrogen and carboxylic (Fukumoto et al., 2005). Glutamic acid or its salt is an amino acid containing more than one carboxylic group. Starting synthesising solid scale dissolver from glutamic acid or its salt will reduce the synthesis step in adding a carboxylic group to the dissolver. In addition, glutamic acid salt is available in abundant in the market at a cheap cost. This advantage makes glutamic acid as interesting starting materials for the development of amino acid solid scale dissolver.

1.2 Problems Statement

In oil and gas production, solid scale formation comes from solid precipitation or crystallisation of dissolved salt or mineral compound in a various part of production including reservoir, production well perforation, well tubular and piping (Bhaduri et al., 2018; Chen et al., 2016; Merdhah & Yassin, 2007; Muryanto et al., 2014). This precipitation may grow to the extent disrupting oil and gas operations such as blocking wellbore tubes. Scale formation may directly block the flow of the well either in the well tubular or the permeability of the reservoir (Mackay, 2007). Scale formation in the piping system may lead to valve failure, corrosion of pipe or tube surface underneath the scale, restriction or blockage of the flow or damaging the equipment (Abass et al., 2002; Crabtree et al., 1999)

The solid scale formation had caused a significant cost spending for oil production (Crabtree et al., 1999; Jordan et al., 2001; Tjomsland et al., 2013). Among the operational cost involved are well enhancement and scale dissolution (Crabtree et al., 1999; Jordan et al., 2001). The study shows a total of 6.3 million USD had been spent from 1993 to 1999 for scale control operation at Veslefrikk field, Norway. It was estimated that, in a similar timeframe, 9 million Sm^3 less oil will be produced, representing a reduction in cash flow approximately 1100 million USD, at the time of estimation (Tjomsland et al., 2013). The cost of cleaning out the single well and putting it back on production was approximately the same as the chemical costs to treat the entire field (Wigg & Fletcher).

One of the most common scale in an oil well is calcium carbonate (Jasinski et al., 2013; Muryanto et al., 2014; Vetter & Farone, 1987; F. Zhang et al., 2017) The loss of CO_2 in the formation water due to drop of pressure remove carbonate acid that keeps the calcite dissolved (Ramstad et al., 2005; P. Zhang et al., 2015). Acid is commonly used to dissolve calcium carbonate scale or to improve the permeability of the well. However, acid treatment is known to cause significant damage to the well tubular and other equipment due to their corrosive properties (Di Lullo & Rae, 1996; Olajire, 2015; P. Zhang et al., 2015). Barium sulphate is the most insoluble scale that can be precipitated from oilfield waters. It forms a hard scale which is extremely difficult to remove (Bageri et al., 2017; Vetter, 1975). The solubility of barium sulphate goes up with increasing temperature, pressure and salt content of the brine (Crabtree et al., 1999; Merdhah, 2007; Vetter, 1975). Barium sulphate scale is among the toughest scales to remove, whether

mechanically or chemically (Crabtree et al., 1999; Dunn & Yen, 1999). (Bageri et al., 2017)

In solid scale dissolution, new generation dissolver utilised special functional group such as amino acid in their dissolution mechanism. Amino acid contains carboxylic group and amine that can act as ligand to bond with metal ion in solid scale. Dissolver containing carboxylic and amine can reduce the reprecipitation of solid scale. However, there is lack of understanding on the intermolecular interaction between the important functional group; carboxylic and amine with the metal ions in the solid scale. In this study, monosodium glutamate (MSG) is used as main reactant for the synthesis of amino acid based solid scale dissolver. MSG is non-toxic and environmentally friendly compound often used in food processing containing two carboxylic and one amine group. MSG is available in abundant and low cost makes it attractive to be used to synthesised amino aicd base ionic liquid for solid scale dissolver application.

1.3 Research Objectives

The main objective of this study is to develop the new solid scale dissolver from monosodium glutamate for application in oil well intervention for dissolution of calcium carbonate and barium sulphide. This study will also involve the dynamic simulation of a chelating agent; glutamic acid diacetic acid (GLDA) and glutamic acid diacetic acid tetrasodium salt (GLDA-Na_4) used in dissolving calcium carbonate and iron sulphide. Simulation of intermolecular interaction will gain a fundamental understanding of the main role of the main functional groups in the solid scale dissolution. Within this overall context, the objectives of this study are:

1. To synthesise and characterise the amino acid-based solid scale dissolution from monosodium glutamate. Monosodium glutamate is a poly-amino carboxylic acid salt containing two carboxylic and one amine group.
2. To evaluate the dissolution of calcite ($CaCO_3$) and barite ($BaSO_4$) solid scale using synthesised amino acid-based solid scale dissolver.

CHAPTER 2

LITERATURE REVIEW

2.1 Introduction of Chapter

This chapter provides a theoretical background of fundamental knowledge for this study. The first part will be a review about solid scale formation in upstream oil and gas production, the mechanism of solid scale formation and targeted solid scale selected for this study; calcium carbonate, barium sulphate and iron (II) sulphide. Introduction regarding reservoir and oil and gas well intervention has been explained. The third part of this chapter will review about theoretical background of molecular dynamic simulation followed by literature for amino acid based solid scale dissolver.

2.2 Oil and Gas Reservoir

Petroleum reservoir is a subsurface layer of permeable and porous rock containing oil or natural gas surrounded by impermeable rock. This is the layer where the oil, gas or water may accumulate and trapped or may even be dry (Economides, 2012; Terry & Rogers, 2014). The petroleum from inside the reservoir when organic material accumulated and trapped between impermeable rock layer either through rock deformation or natural formation of an impermeable layer on top of the sedimentation. This trapping exerts pressure and heat on the organic material transforming it into hydrocarbon (Ezekwe, 2010).

2.2.1 Reservoir Structure

The most common sedimentary rock or reservoir rock are sandstone, carbonates, and shale. Reservoir rock fundamental components are grains (sand or fossil), matrix (fine grain or clay sediment), cement (minerals precipitation) and porosity (space with no minerals). Space or porosity will act as a storage of crude oil or gas as well as water

(Terry & Rogers, 2014). Type of rock in the reservoir will determine the type of scale possibly forming during oil and gas extraction. Water in the reservoir usually contains a significant concentration of dissolved minerals. External disturbance such as brine injection in oil production will cause these minerals to precipitate and forming scale (Nassivera & Essel, 1979; Read & Ringen, 1982; Vetter et al., 1982).

2.2.2 Oil and Gas Well Stimulation and Intervention

Any activities or work is done on oil or gas well near or at the end of its production life to improve the production rate is regarded as well intervention (Houseworth, 2013). In some cases, well intervention might be used interchangeably with well stimulation. Well stimulation refers to a range of activities to increase production by improving reservoir permeability, not restricted to well at its end of production life. Stimulation may be done when there are damages caused by drilling or blockage caused by scale formation or mineral precipitation, sand production or perforation damage (Economides, 2012; Ghalambor & Economides, 2002; Houseworth, 2013).

Mechanical disturbance during drilling and chemical reaction with drilling fluid may plug reservoir pores, migration of fine particles or swelling of the clays that eventually lead to a reduction of permeability (Ghalambor & Economides, 2002). Depletion of oil in a reservoir forced extra effort to be carried out to improve production or to recover remaining oil. Intervention might involve work as simple as pumping the oil, slickline operation for fishing, gauge cutting, and blockage removal, or coiled tubing for pumping chemical and fluid into the well. Three most common well stimulation technique are hydraulic fracturing, acid fracturing and matrix acidizing (Čikeš, 1996; Economides, 2012; Oloro et al., 2010). The new well stimulation and scale control are utilising chelating agent (Mohamed A. Mahmoud, Nasr-El-Din, De Wolf, LePage, & Bemelaar, 2011).

2.3 Solid Scale in Oil Production

Well flow may be reduced or stopped due to several factors including a reduction in the well pressure, blocking of reservoir pore near the drainage area and scale formation in a

wellbore that blocks the flow of the fluid (Ghalambor & Economides, 2002). This problem often contributed by solid deposition comes from the inside of the reservoir itself (Crabtree et al., 1999). Well completion involved pumping of high-pressure drilling fluid into the wellbore that probably damages the surrounding formation in the reservoir. This damage will introduce solid particle such as sand and clay into the reservoir pores and reduce the oil flow towards the drainage area or block the drainage area itself (Economides, 2012).

2.3.1 Mechanism Solid Scale Formation

The solid scale is the formation of solid sedimentation or crystallisation of dissolved salt or mineral compound in liquid. In oil and gas production, precipitation or deposition of dissolved solid commonly inorganic salt from aqueous solution in well tubular will caused the formation of scales (Kelland, 2014). Oilfield scale might contain several minerals, sand, organic precipitates, wax as well as corrosion product (Mackay, 2007). This precipitation may growth to the extent disrupting oil and gas operations such as blocking wellbore tubes. Scale formation in the piping system may lead to valve failure, corrosion of pipe or tube surface underneath the scale, restriction or blockage of the flow or damaging the equipment (Crabtree et al., 1999; Merdhah, 2007; Merdhah & Mohd Yassin, 2009).

Aggregation of deposit that cake the production well perforation, casing and tubing as well as valve and other downhole completion equipment will also lead to scale formation that will completely block the flow of the liquid. Similar to scale forming in home plumbing, over time, the deposition or crystallisation will grow to form a thick lining on the tubular surface, thereby reduce the flow and eventually completely block it (Crabtree et al., 1999). One of the recorded scale problems is in the North Sea, Miller field where scale causes the production fall from 4770 m^3/d to zero in just 24 hours. Such case shows how severe scale problem can affect oil and gas production (Brown, 1998).

Figure 2.1 below shows solid scale formation. The location of scale deposits in the tubing can vary from downhole perforations to the surface where it constrains production through tubing restrictions, blocked nipples, fish, safety valves and gas-lift mandrels. The scale is often layered and sometimes covered with a waxy or asphaltene

coating. Pitting and corrosion on steel can develop under the scale due to bacteria and sour gas, diminishing steel integrity (Crabtree et al., 1999).

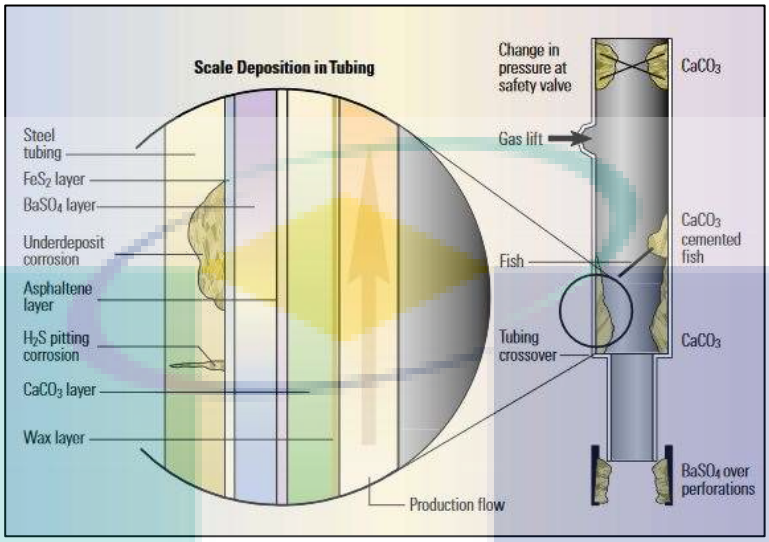

Figure 2.1 Scale formation in the tubing.
Source: Fighting Scale-Removal and Prevention (Crabtree et al., 1999).

The main source of scale is from the reservoir itself. However, the scale will only form if water is produced or injected into the well. Some minerals are readily dissolved in the produced water, full of ions such as Ca^{+2}, Mg^{+2}, Ba^{+2} and Sr^{+2}. Alteration of reservoir formation such as improving permeability will increase the concentration of dissolved minerals until it reaches its saturation limit (Nassivera & Essel, 1979; Read & Ringen, 1982; Vetter et al., 1982). Mechanism and factors contributing to scale formation are various, among others are changed in temperature and pressure. Well production and completion involving fracturing and permeability enhancement cause a significant change in temperature and pressure (Mackay, 2007; Moghadasi et al., 2007). The dissolved mineral originally exists in the produced water added with salt form the brine injection may precipitate when the temperature and pressure changes.

It is estimated that dissolve solid in reservoir fluid may reach up to 400, 000 mg/L (Crabtree et al., 1999). When changes on this fluid occur either by production or stimulation, such as solubility of one or more components exceeded the saturation limit, the scale starts to form. This formation highly depends on temperature and pressure as the solubility of dissolved solid changes with changes of those two factors (Crabtree et al., 1999). The first step in solid scale formation is homogeneous nucleation of an

unstable atom in the saturated fluid. This unstable atom starts forming the crystal seed cause by equilibrium inconstancy of ion concentration in the supersaturated liquid as shown in Figure 2.3. In a simple explanation, the seed crystal will be a catalyst for scale formation. This seed later starts to growth, consequently increase in size. This process closely related to the critical radius of the crystal growth. After the critical radius exceeded, the surface free energy decrease drives the growth energy (Crabtree et al., 1999; McSween et al., 2004; Mullin, 2001).

Heterogeneous nucleation usually initiated on existing fluid boundary surfaces include a surface defect, roughness, perforation, joint ad seams in tubing or pipelines. Figures 2.3 shows the heterogeneous nucleation of scale crystal on the surface of tubing due to surface imperfection. A high degree of turbulence can also catalyse scale deposition. Thus, the accumulation of scale can occur at the position of the bubble point pressure in the flowing system. This explains why scale deposits rapidly build on downhole completion equipment. Given the high degree of saturation in the produced water in the reservoir, the seed crystal encourages the growth of a solid scale (Crabtree et al., 1999).

Some of the most common scale minerals are wax, calcium carbonate (calcite, aragonite, and vaterite), barium sulphate (barite), iron (ii) sulphate, and silicon dioxide (sandstone). Some other types of scales are calcium sulphate (anhydrite and gypsum), strontium sulphate (celestine), mackinawite (Fe-S-Ni), pyrite (FeS2), Halite (NaCl), Fluorite (CaF2), Sphalerite (Zn, Fe, S) and Galena (PbS) (Crabtree et al., 1999; Merdhah, 2007; Merdhah & Mohd Yassin, 2009; Nasr-El-Din & Al-Humaidan, 2001; Vetter & Farone, 1987; Vetter et al., 1982)

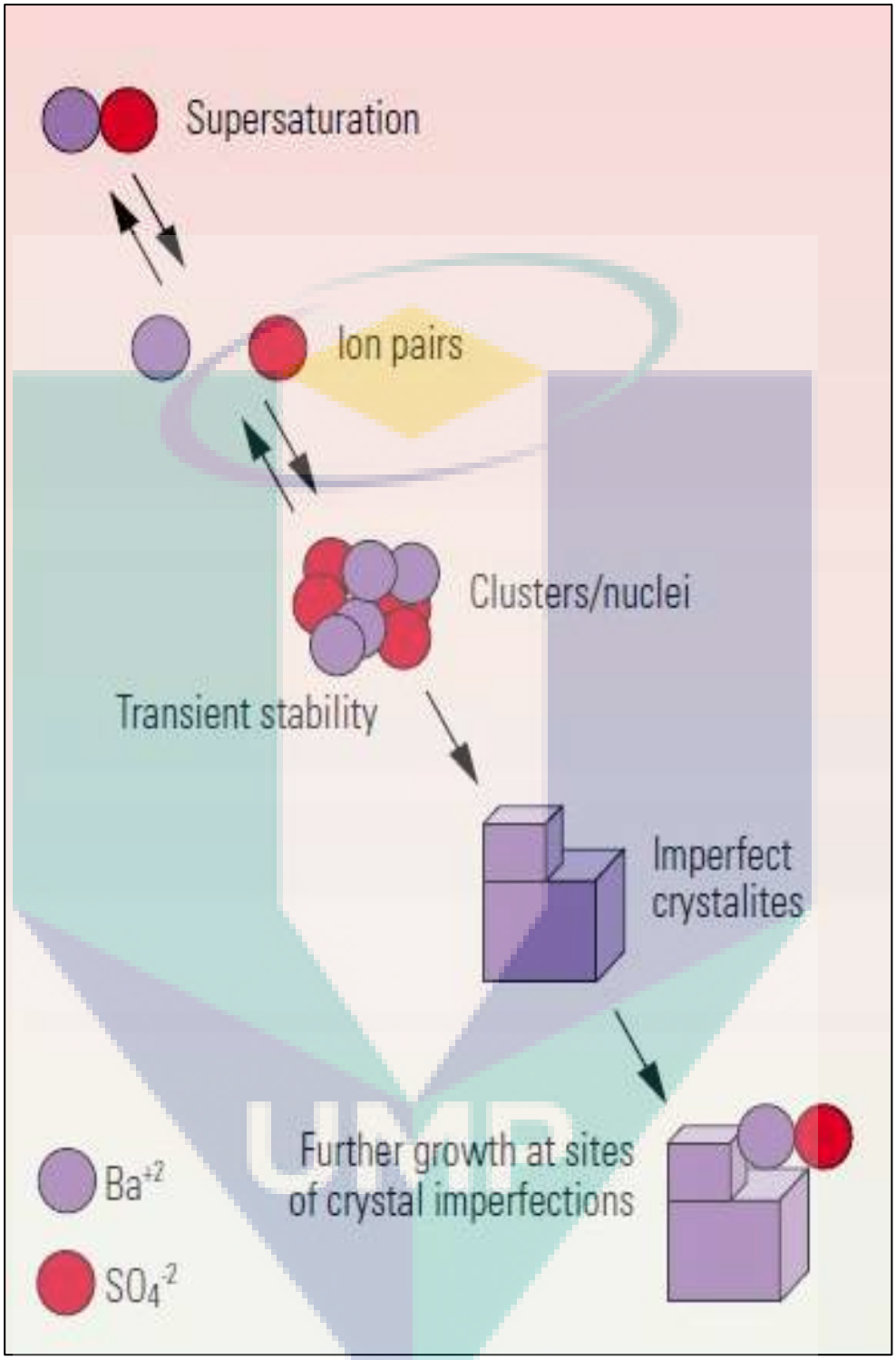

Figure 2.2 Homogenous nucleation of supersaturated solution becoming seed crystal and growth to become a solid scale.

Source: Fighting Scale- Removal and Prevention (Crabtree et al., 1999).

.

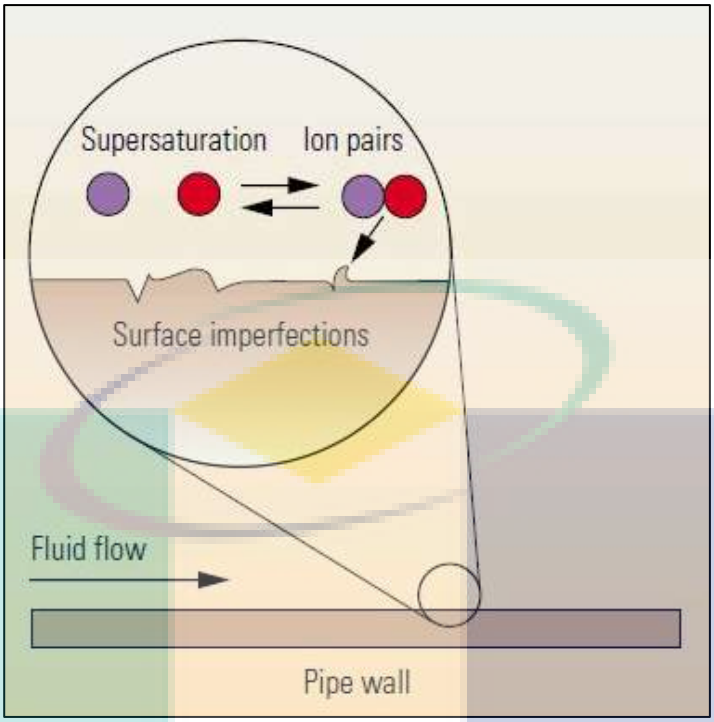

Figure 2.3 Heterogenous nucleation of solid scale crystal on surface imperfection. Source: Fighting Scale-Removal and Prevention (Crabtree et al., 1999).

2.3.2 Calcium Carbonate Scale

Calcium carbonate scale is one of the most common scales in oil and gas industries especially in well tubular (Vetter & Farone, 1987). The saturated calcium carbonate aqueous solution in the well mixed with incompatible water from well injection cause crystallisation of carbonate and start forming scale (H. A. Nasr-El-Din, Al-Saiari, Al-Ruwaily, & Al-Gamber, 2006). The loss of CO_2 in the formation water due to drop of pressure remove carbonate acid that keeps the calcite dissolved (Ramstad, Tydal, Askvik, & Fotland, 2005; O. J. Vetter et al., 1982). This led to precipitation of calcite from salt-forming ions (calcium ions). At high temperature, calcium carbonate solubility is significantly reduced (Weyl, 1959). Formation of calcite scale likely occurs follows chemical Equation 2.1 below:

$$Ca^{+2} + CO_3^{-2} \rightarrow CaCO_3 \qquad 2.1$$

Commonly hydrochloric acid at 5-15% concentration is used to dissolve calcite in well under most conditions (Connell, 1983). However, the chelate agent was also utilised to control the solid scale as it can dissolve and prevent the reprecipitation of the

solid scale. The dissolution mechanism of calcite with acid and chelate agent, ethylenediaminetetraacetic acid (EDTA) are represented in chemical Equation 2.2 and 2.3 (Lepage et al., 2011):

$$CaCO_3 + 2HCl \rightarrow H_2O + CO_2 + CaCl_2 \quad 2.2$$

$$EDTA^{4-} + CaCO_3 \leftrightarrow [EDTA - Ca]^{2-} + CO_3^{2-} \quad 2.3$$

2.3.3 Barium Sulphate

Barium sulphate is the most insoluble scale that can be precipitated from oilfield waters. Barium forms a hard scale which is extremely difficult to remove once precipitated (Vetter, 1975) The solubility of barium sulphate goes up with increasing temperature, pressure and salt content of the brine (Crabtree et al., 1999; Vetter et al., 1982). Barium sulphate scale is among the toughest scales to remove, whether mechanically or chemically (Crabtree et al., 1999; Dunn & Yen, 1999). However, chemicals based on EDTA and diethylenetriaminepentaacetic acid (DTPA) are now available which have had some success in dissolving barium sulphate (Bageri et al., 2017; Dunn & Yen, 1999). Equation 2.4 shows the chemical equation of barium sulphate formation (Merdhah & Yassin, 2007). Most of barium ions and sulphate originated from the formation of water itself. Mixing of incompatible brine solution often causes the deposition of $BaSO_4$ (Crabtree et al., 1999).

$$Ba2+ + SO42+ \rightarrow BaSO4 \quad 2.4$$

2.4 Ionic Liquid

Ionic liquid (IL) is a molten salt with melting point below 100 °C. Pure IL will consist of cations and anion with high degree of asymmetry (Brennecke & Maginn, 2004).

2.4.1 Ionic Liquid in Oil and Gas

Despite its versatility, application of IL in oil and gas in upstream, midstream or upstream are still at early stage of laboratory study. The unique properties of IL can be promising to be used in a various stage in petroleum industries. Several laboratory studies have successfully utilised ionic liquid 1-ethyl-3-methyl- imidazolium tetrafluoroborate

([Emim][BF4], to recover bitumen from oil sand. This mainly contributed by the changes of the adhesive force between bitumen and silica after IL addition due to its unique behaviour at the surfaces and the charged interface resulting from the high ion concentration. (Li et al., 2011; Painter, Williams, & Mannebach, 2010). A study by Nares et al., (2007) shows the hydrogenation and hydrocracking ability of iron-base and molybdenum ionic liquid can be used for upgrading heavy crude oil in mild operating condition. The polar molecules of the heavy crude oil probably would be diffused in ionic liquid favouring the contact between both phases and the metals compounds in the ionic liquid have been recognised because of their catalytic properties in hydrocarbon oxidation, cracking, and hydrocracking reactions (Nares et al., 2007).

In addition, Ammoeng (acrylic ammonium base) ionic liquid shown the promising result to be applied as a surfactant in enhanced oil recovery by affecting the interfacial tension between reservoir fluid (Benzagouta, AlNashef, Karnanda, & Al-Khidir, 2013; Lago et al., 2013). Other studies also proved the potential of ammonium and phosphonium ionic liquid to be used in enhanced oil recovery (Bin-Dahbag et al., 2013; Bin Dahbag, AlQuraishi, & Benzagouta, 2015; Pereira, Costa, Foios, & Coutinho, 2014). However, the studies of the ionic liquid for enhanced oil recovery choose a different type of ionic liquid and still at early stage making comparison difficult. In this study, the glutamic based ionic liquid has been chosen as the based due to the presence of carboxyl and amine functional group in the structure believed to plays important role is solid scale dissolution.

2.4.2 Amino acid based Ionic Liquid

The ionic liquid to be produced in this study is aimed to be biodegradable and environmentally friendly. Common quaternary nitrogen based ionic liquid such as alkylammonium, dialkyl imidazolium and pyridium are synthetic, thus not as green as desired (Tao, He, Sun, & Kou, 2005). Therefore, the amino acid is chosen as the main based of the ionic liquid as amino acid and their derivatives are the most abundant natural source of quaternary nitrogen precursor. The similar amino acid based, monosodium glutamate is also used in producing GLDA, and prove to be biodegradable and environmentally friendly (Mahmoud et al., 2011).

Other than nitrogen, chelating agents used in solid scale control commonly contains a notable number of carboxylic group that will act as a ligand in chelating the metal ions (Mahmoud et al., 2011; Moghadasi et al., 2007; Sillanpaa & Oikari, 1996). All amino acid contains both nitrogen and carboxylic, however, glutamic acid or its salt and aspartic acid contain more than one carboxylic group. Starting synthesising ionic liquid from glutamic acid and aspartic acid will reduce the synthesis step in adding a carboxylic group to the ionic liquid. Figure 2.7 shows the structure of L-glutamic acid and L-aspartic acid.

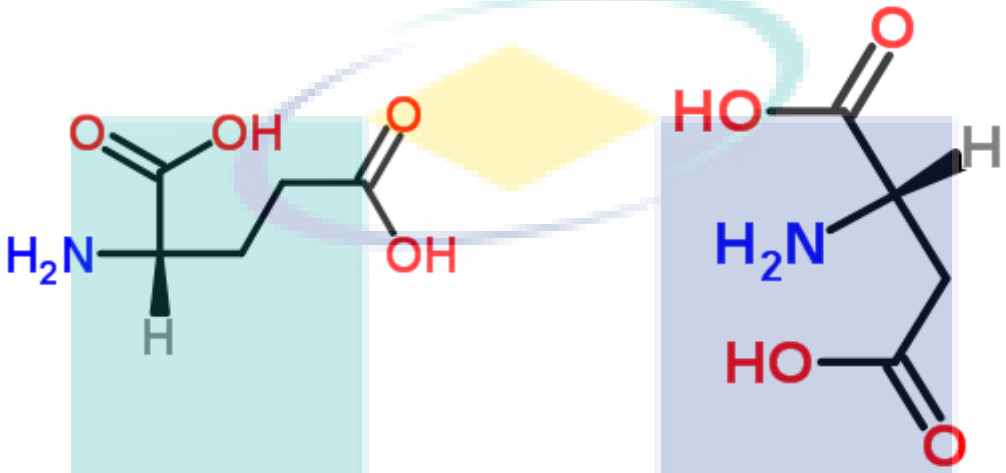

(a) (b)

Figure 2.7: Molecular structure of (a) L-Glutamic acid and (b) L-Aspartic acid.
Source: L-Glutamic Acid (Chemspider, 2017d) and L-Aspartic Acid (ChemSpider, 2017c)

2.4.3 Synthesis of Ionic Liquid

The synthesis route chosen for glutamic based and fluorine ionic liquid involve alkylation of glutamic acid to produce chloride salt using 1-chlorobutane or iodine salt using nonafluoro-1-iodobutane. Alkylation function to reduce hydrogen bond from the carboxylic group in the glutamic acid thus lower the melting point of the final product (Tao et al., 2005). The sodium tetrafluoroborate or sodium hexafluoro borate will be used next for metathesis reaction to replace chloride ion with new anion containing fluorine as one of the functional group. This route adapted from Gupta et al. (Gupta, Armstrong, &

Shreeve, 2003) for the production of quaternary trialkyl (poly fluoroalkyl) ammonium salts and Tao et al. (Tao et al., 2005) for the production of amino acid based ionic liquid

2.5 Amino Acid Based Solid Scale Dissolver

2.5.1 Functional Group of Amino Acid

The amino acid is an organic compound determine by the existence of carboxylic (-COOH) and amine (-NH_2) as its primary functional group with other functional group attached to its side chain. The structure contains a central carbon atom in which both amine and carboxylic is attached to as shown in Figure 2.6 (a). In most cases, amino acids exist as crystalline solids. At neutral pH values, carboxylic group the carboxylic group will deprotonate, and amine will be protonated forming a zwitterion (Figure 2.6 (b)).

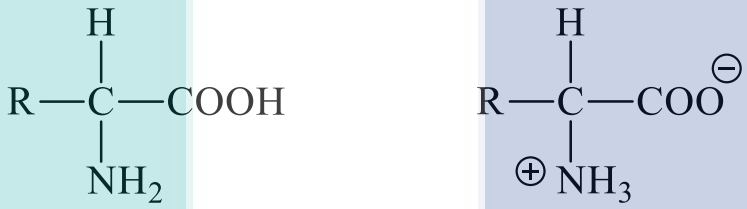

(a) (b)

Figure 2.4 (a) General chemical formula of an amino acid with carboxylic and amine both attached to the same carbon and (b) zwitterion of carboxylic acid.

In this study, monosodium glutamate (MSG) is used as the main material for the synthesis of amino acid based solid scale dissolver. MSG is the sodium salt of L-glutamic acid, the most abundant amino acid naturally occurs in nature. Synthetic MSG is widely used as flavour enhancer produces mainly through the fermentation process of plant sources carbohydrates such as sugar cane and tapioca. MSG often comes in the form of monohydrate crystal with a molecular weight of 187.127 g/mol. Figure 2.7 shows the molecular structure of MSG. MSG contains two carboxylic groups, one of which in its carboxylate form with sodium atom and one amine group.

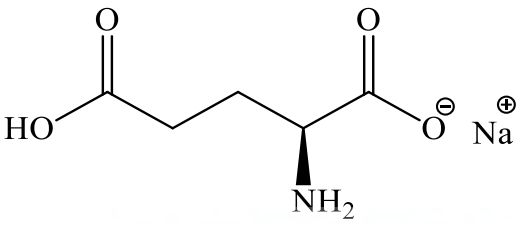

Figure 2.5 Molecular structure of monosodium glutamate (MSG). MSG contains one carboxylic group, one carboxylate ions and amine connected to the carbon chain.

2.5.2 Acidification of Amino Acid

Acidification of amino acid is a protonation reaction carried out by mixing correct molar ratio of an amino acid with a strong acid such as hydrochloric acid in water followed by the evaporation of water (Tao et al., 2005). This reaction will protonated amine group of amino acid forming an amine salt. The general reaction mechanism for acidification of amino acid is represented in Figure 2.8. For amino acid containing carboxylate, the carboxylate ions will first be protonate forming salt as a by-product (Borissova et al., 2005).

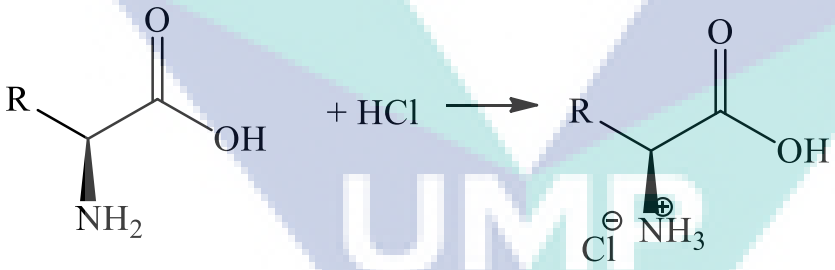

Figure 2.6 General reaction mechanism for acidification of amino acid.

2.5.3 Metathesis of amino acid salt

Metathesis is a chemical process involving the exchange of bonds between two non-reacting chemical species which results in the creation of products with similar or identical bonding affiliations (Gao et al., 2005; Gupta et al., 2003; Tao et al., 2005). The bond between the reacting species can be either ionic or covalent. Metathesis is a common technique for exchanging counterions especially in the synthesis of ionic liquid (Xue et al., 2006). In amino acid based solid scale dissolver, amino acid chloride salt form acidification is metathesis with a metal

salt. The general reaction schemed is showed in Figure 2.9. The metals salt choose in the reaction will consist of the cation of preferably choice to be included in the final product.

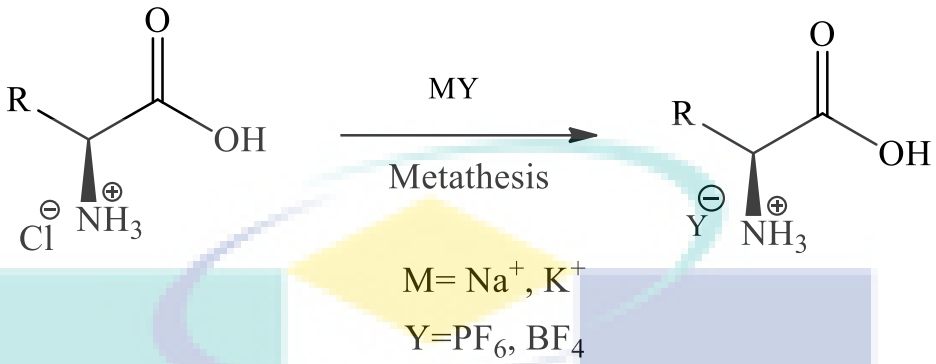

Figure 2.7 General reaction mechanism for the metathesis of amino acid salt with metals salt.

2.6 Summary

This chapter provides a literature review necessary for this study. The literature review includes the introduction of well interventions method that becomes the main direction of this study, to develop ionic liquid for solid scale dissolution in well intervention. Small information regarding oil and gas reservoir is also included to understand more on the origin of the solid scale itself. Second part review about the mechanism of solid scale formation and targeted solid scale selected for this study calcium carbonate and barium sulphate. The third part of this chapter reviews about the theoretical background of molecular dynamic simulation followed by literature regarding amino acid solid scale dissolver.

CHAPTER 3

METHODOLOGY

3.1 Synthesis of Amino Acid based Solid Scale Dissolver

3.1.1 Materials

The materials brand and purity of all chemicals used in this experiment are listed in Table 3.2 below.

Table 3.1 List of materials, its brand and purity used in acidification of monosodium glutamate

Materials	Brand	Molecular Weight (g/mol)	Purity
Monosodium glutamate	Ajinomoto	169.111	99%
Hydrochloric acid	HmbG Chemicals	36.46	37%
Tetra fluoroboric Acid	Sigma Aldrich	87.81	48 wt%
L-Glutamic Acid (Standard)	Sigm Aldrich	147.130	98.5-100%
Sodium Hexafluorophosphate	Sigma Aldrich	167.954	98%
Sodium Fluorophosphate	Sigma Aldrich	143.95	95%
Sodium Trifluoro methane sulfonate	Sigma Aldrich	172.06	98%

3.1.2 Precipitation of Glutamic Acid from Acidification of Monosodium Glutamate

The main materials used in acidification is monosodium glutamate, hydrochloric acid and hydro fluoroboric acid. In the acidification of MSG, 33.822 g of MSG (0.2 mol) was dissolved in 150 ml of deionised water. The solution was continuously stirred using magnetic stirrer as shown in Figure 3.1. About 16.56 ml of 37% HCl was added drop by drop into the solution and the white precipitate (glutamic acid) will start to form. An

excess of 2 ml of HCl was then added. The mixture was continuously stirred 10 minutes. The stirring was stopped and the glutamic acid allowed to precipitate for 12 hours.

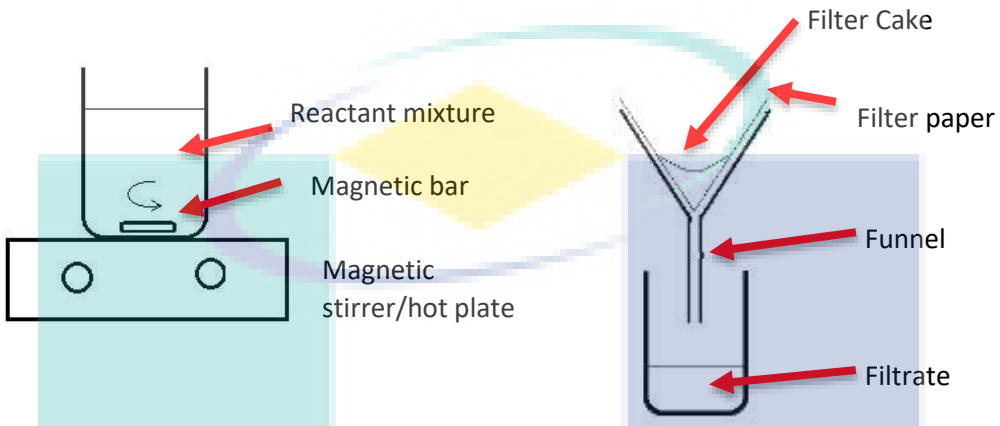

(a) (b)

Figure 3.1 General experimental set-up for (a) acidification and metathesis and (b) filtration for separation of product

Once a supernatant can be observed, the water was separated by carefully pouring about 2/3 water from the supernatant and retaining the solid inside the beaker. Then, 100 ml of deionised water was added to wash the glutamic acid and allowed to precipitate again for another 30 minutes. Once a supernatant can be observed, the water was separated again by carefully pouring out the liquid. This process was repeated for three times. The remaining liquid after the third washing was separated using filter paper as shown in Figure 3.1(b). The glutamic acid collected was dried in an oven at 60 ˚C until a constant weight was obtained (24-48 hours). The dried glutamic acid was weight to determines it's yield before analysed using Fourier transform infrared (FTIR) and compare with standard glutamic acid purchased from Sigma Aldrich. The yield of the product was calculated using the formula below.

$$Yeild = \frac{Experimental\ Product\ Mass}{Theoritical\ Product\ Mass}\ x\ 100\% \qquad 3.2$$

3.1.3 Glutamic Acid Hydrochloride from Acidification of Glutamic Acid

Glutamic acid produced from the first acidification can be further acidified to produce salt with chloride or fluoroboric as an anion and glutamic as the cation. The acidification of glutamic acid will protonate the amine group (Rong et al., 2008; Tao et al., 2005). About 29.426g of glutamic acid from the first acidification was mix with 100 ml of deionised water and continuously stirred using the magnetic stirrer to break all large pieces of the glutamic acid. Once a homogeneous mixture was obtained (white milky colour) about 16.56 ml of hydrochloric acid was added drop by drop to the mixture. The mixture will turn into a colourless solution. The solution was then continuously stirred for 1 hour. If any undissolved solid was observed, the solution will be filtered with filter paper. The solution was evaporated under vacuum using rotary evaporator at 60 °C until all the liquid has evaporated. The solid product was collected and transferred into a beaker and then dried in a vacuum oven at 60 °C until the mass of the product remains constant (24-48 hours).

3.1.4 Glutamic Acid Tetrafluoroborate from Acidification of Glutamic Acid

For acidification of glutamic acid using tetra fluoroboric acid (HBF_4), the similar steps were followed in Chapter 3.3.3. About 29.426g of glutamic acid from the first acidification was mix with 100 ml of deionised water and continuously stirred using the magnetic stirrer to break all large pieces of the glutamic acid. Once a homogeneous mixture was obtained (white milky colour) about 26.134 ml of tetrafluoroboric acid was added drop by drop to the mixture. The mixture will turn into a colourless solution. The solution was then continuously stirred for 1 hour. If any undissolved solid was observed, the solution will be filtered with filter paper. The solution was evaporated under vacuum using rotary evaporator at 60 °C until all the solution turns into viscous liquid (1-2 hours). The liquid was transferred into a beaker and then placed in a vacuum oven at 60 °C until the mass of the product remains constant (48-72 hours). The yield was calculated using formula 3.1.

3.1.5 Metathesis of Glutamic Acid Hydrochloride

Glutamic acid hydrochloride 0.1 mol (20.557 g) was dissolved in 150 ml of deionised water and continuously stirred until all the solid dissolved. An equimolar amount of sodium trifluoro methanesulfonate (17.206 g) salt was added into the solution and stirred for 48 hours. Then, the solution was filtered using filter paper (Figure 3.1(b)) to separate undissolved solid, if any. The filtrate was evaporated using rotary evaporator at 60 °C until it turns into a viscous liquid with solid precipitation observed (1-1.5 hours). 30 ml of acetone was poured into the evaporating flask to wash the product. The solid will remained precipitated. The mixture was then filtered using filter paper to separate the solid. A small amount of acetone (2-3 ml) was used to wash the solid during filtration. The filtrate was slowly evaporated at 60 °C for 2 hours. The washing process using acetone was repeated and any precipitate was separated using filter paper. The filtrate was evaporated again at 60 °C for 2 hours then transferred into a vacuum oven at 60 °C until the constant mass of product was obtained (24-48 hrs).

3.2 Dissolution Test

Dissolution of calcium carbonate ($CaCO_3$) and barium sulphate ($BaSO_4$) with a solution of the product from the reaction in Chapter 3.3.3. 3.3.3, and 3.3.4 was performed. $CaCO_3$ (99%) was supplied by Sigma Aldrich in the form of a powder and $BaSO_4$ (98%) was supplied by Acros Organic in the form of fine powder. The concentration of the solution of the product from the reaction was fixed at 20g/L but was varied in pH from acidic (<3), pH 6.5-7 and alkaline (>10). 0.1 Molar of HCl and KOH was used as buffer solution adjust the pH of the solution. Dissolution was conducted by adding 2 g of $CaCO_3$ and $BaSO_4$ to 40 ml of the solution at 60 °C for 24 h. The mixture was then filtered to separate the undissolved solid scale. The filtrate was analysed using Perkin Elmer Optima 8000 inductively coupled plasma optical emission spectrometry (ICP-OES) to determine the concentration of total dissolved metal (Bageri et al., 2017; Lepage et al., 2011; M. A. Mahmoud et al., 2011).

3.3 Characterisation Analysis

3.3.1 Fourier Transform Infrared Spectroscopy

In a sample preparation for Fourier Transform Infrared Spectroscopy (FTIR), the solid sample (materials or product) was dried and ground into fine particles. All solid and liquid samples were analysed without pre-treatment using Perkin Elmer Spectrum 100 FTIR (United State). Transmittance (%) measurement was carried out from 400 to 4000 cm^{-1} wavelength range for 32 scans at a resolution of 2 cm^{-1}

3.3.2 Molecular Structure Determination

The molecular structure of some of the raw material was characterised by analysing using nuclear magnetic resonance spectroscopy through carbon 13 detection. About 5 mg of the sample was dissolved in 500 µL of deuterium oxide (D_2O) and placed inside the sample tube and analysed using Bruker Ultra Shield Plus 500MHz NMR (United State). The sample was scan for 300 scan number.

3.3.3 Thermal Stability Analysis

Differential Scanning Calorimetry (DSC) was used to study the temperature and heat flow associated with the transition of the material of the synthesis product. Approximately 5-6 mg of product was sealed into aluminium pan and lid and analysed using Perkin Elmer DSC 8000 (United State). The sample was analysed at a rate of 10 °C/min from 30°C to 300 °C with nitrogen gas flow rate purging maintained at 20 ml/min.

3.3.4 Melting Point Analyser

The melting point of the solid sample in this study was analysed using Buchi Melting Point M-565 (Switzerland). The solid sample was ground to a fine powder using mortar and pestle. Three capillary tubes were pressed into the solid powder. The powder was moved to the bottom of the tubes by gently and repeatedly pounding the tube against

a hard base. All tube was filled to the same height of the sample (4-5 mm). The temperature range was set from 60 °C to 250 °C at a heating rate of 10 °C/min.

3.3.5 Elemental Analysis

Perkin Elmer Optima 8000 (United State) inductively coupled plasma optical emission spectrometry was used in this study to determine the concentration of calcium and barium ions in the solution of the product after the dissolution test. A calibration curve of the standard solution was prepared at concentration 0 ppm, 5ppm, 10 ppm and 15 ppm. The sample was filtered using a 0.4-micron nylon filter and diluted to 1000 times using ultrapure water before subject to ICP-OES analysis. The final concentration of metals ions was determined in ppm.

Energy-dispersive X-ray spectroscopy was used to determine the composition of the metal of solid scale and elemental composition of the product. It was done using Hitachi Tabletop Microscope TM3030Plus (Japan) that was equipped with Energy Dispersive X-ray Spectrometer. A small amount of sample was placed on the sample holder using carbon double tape. The sample holder was placed inside the vacuum chamber and the vacuum was started. The EDX analysis was conducted for several point and area to get the average of the elemental analysis percentage.

3.3.6 Surface Morphology Analysis

Surface morphology analysis was conducted using a Hitachi Tabletop Microscope TM3030Plus (Japan) scanning electron microscope. A small amount of sample was placed on the sample holder using carbon double tape. The sample holder was placed inside the vacuum chamber and the vacuum was started. The analysis was done for 500x, 1000x, and 3000x magnification.

3.4 Summary

This chapter provides a general methodology of the work conducted in this study. This chapter summarised all the computational method and experimental work procedure.

Glutamic acid diacetic acid (GLDA) and glutamic acid diacetic acid tetrasodium salt (GLDA-Na_4) was selected for simulation with calcite and ferrite (FeS). Modelling simulation conducted using Material Studio by utilising COMPASS forcefield. Acidification and metathesis reaction was used to synthesise amino acid based solid scale dissolver. From monosodium glutamate.

CHAPTER 4

RESULT AND DISCUSSION

4.1 Solid Scale from Oil Well

Three solid scales have been obtained from oil well referred to as Scale 1 and Scale 2 and Scale 3 respectively. Figure 4.1 below shows the image of a) Scale 1 and b) Scale 2 c) Scale 3. Scale 1 has a yellowish or light brown colour. The layered structure shows that the scale has been crystallised and precipitated layer by layer over a long period of time (Crabtree et al., 1999). Scale 2 has a dark greyish colour with a white patch. Thin layered structure can be seen when the scale is broken into smaller pieces and Scale 2 is significantly more brittles compare to other scales. Scale 3 has a dark brown colour from oil or wax coating, easy to break and have an odour like diesel oil. Once break into smaller pieces, Scale 3 shows white yellowish colour with several thick layers of scale. These thick layers indicate that the solid scale deposited at the wall of the well at a rapid phase.

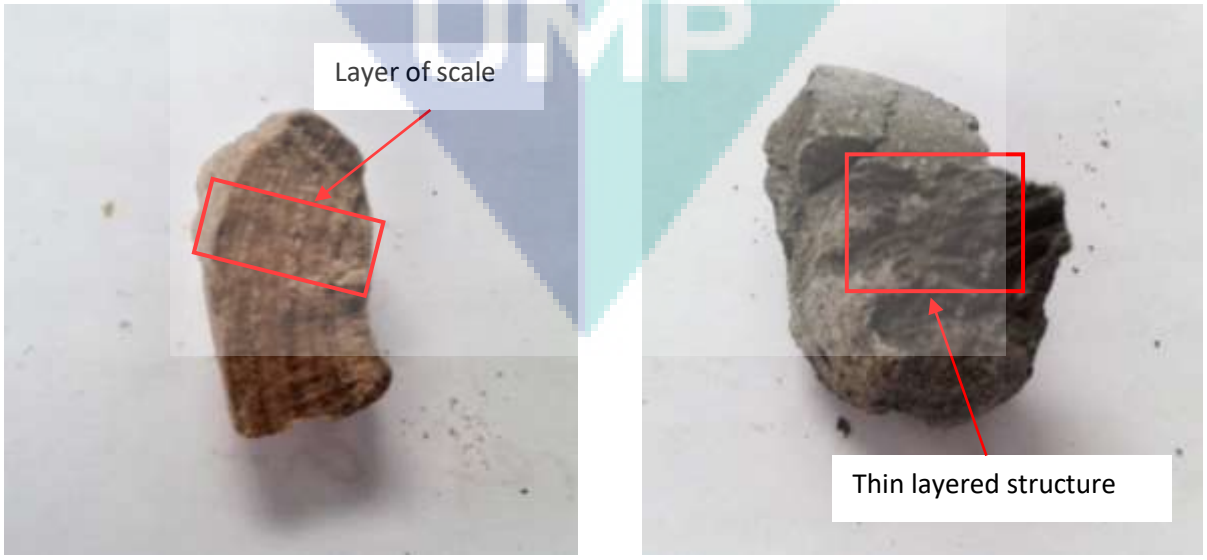

(a) (b)

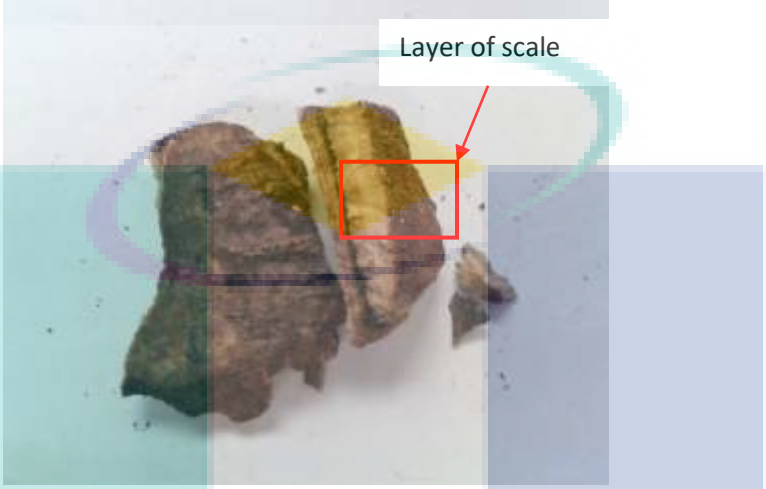

(c)

Figure 4.1 Solid scale obtained from Malaysia offshore oil well (a) Scale 1, (b) Scale 2 and (c) Scale 3

Analysis using Energy Dispersive X-Ray (EDX) gives the composition of atoms available in the solid scale. Table 4.1 shows the composition of Scale 1 form EDX analysis. From EDX analysis, Scale 1 contains mainly barium (43.12 %), oxygen (30.86 %), sulphur (9.57 %) carbon (14.42 %) and strontium (1.37%) with other trace element. The possible minerals present in Scale 1 is barium sulphate ($BaSO_4$), barium oxide (BaO) and strontium oxide (SrO) (Merdhah & Yassin, 2007). The presence of carbon might indicate the trace of hydrocarbon inside the scale that causes the layered structure of the scale to become visible in Figure 5.1 (a) as it deposited over time (Crabtree et al., 1999; Merdhah & Yassin, 2007; Vetter, 1975). Figure 5.2 shows scanning electron microscope (SEM) of Scale 1 at (a) 500x magnification, (b) 1000x magnification and (c) 3000x magnification. SEM image of Scale 1 solid scale shows a crystalline surface; steps, kink, and edge vacancies (Mullin, 2001) that can be associated with crystallisation of barium sulphate. Barium form when incompatible water containing barium and sulphate mix together, caused the nucleation of barium sulphate crystal that will grow becoming a solid scale crystal (Crabtree et al., 1999; Merdhah, 2007).

However, because barium sulphate is not the only component presence, the structure still contains microcrack and porous space that can be seen at 3000x magnification in Figure 4.2 (c). Although porosity and microcrack can be helpful in improving absorption of chemical for scale treatment, $BaSO_4$ is still considered the most difficult solid scale to remove(Dunn & Yen, 1999; Vetter, 1975; Vetter et al., 1982). This is caused by the high purity of barium sulphate scale during crystallisation that creates a layer of very low porosity and impervious to chemical treatment (Crabtree et al., 1999).

Table 4.1 Composition of Scale 1 solid scale from EDX analysis

Elements	**Weight % (%)**	**Minerals Composition**
Ba	43.12 ± 0.424	Barium sulphate, barium oxide and strontium oxide.
O	30.86 ± 0.379	
S	9.57 ± 0.152	
C	14.42 ± 0.486	
Sr	1.37 ± 0.424	

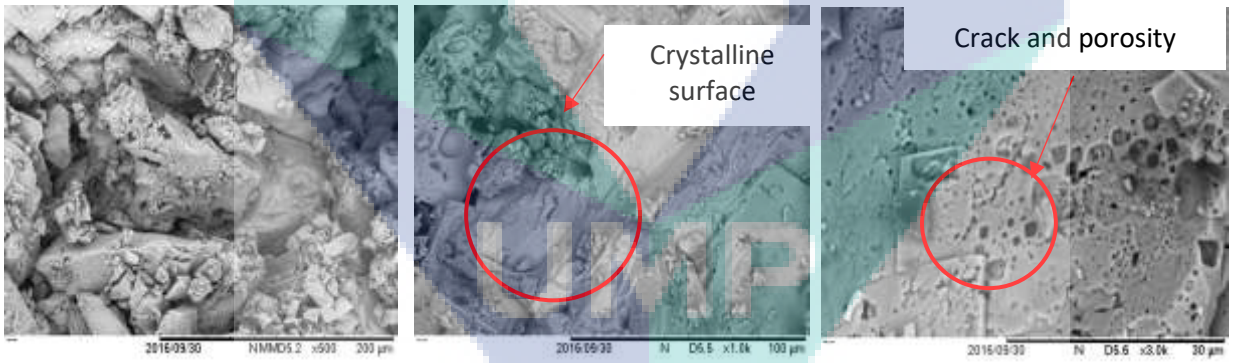

Figure 4.2 SEM image of SCALE 1 solid scale at a) 500x magnification, b) 1000x magnification and c) 3000x magnification.

From EDX analysis in Table 4.2, the main composition of Scale 2 is oxygen and silicon at 55.77 % and 23.52 % respectively. Other element present are aluminium (10.65 %), potassium (3.84 %), iron (2.60 %), calcium (1.54 %) and magnesium (1.02%). Based on this composition, Scale 1 contains silica (SiO_2) and quartz (SiO_2). The present of aluminium and carbon indicate the

possibility of aluminium silicate minerals (andalusite, sillimanite and kaolinite) and a possible trace of calcium carbonate ($CaCO_3$). The high number of silicas indicate that Scale 2 might originate from clay, dissolved sand or very fine sand agglomerated to form a scale (Basbar et al., 2013; Mutnovskoe & Field, 2000). It is still poorly understood on the mechanism of silicate scale deposition. Silica scale formation mechanism likely starts with the dissolution of silica (SiO_2) during matrix acidizing or alkaline flood. When this dissolved silica meets neutral pH water, it will start to form colloidal silica. The presence of metals such as magnesium will bond this colloidal silica and from the amorphous structure eventually grow to become silicate solid scale (Arensdorf et al., 2010). Figure 4.3 shows the SEM image of Scale 2 solid scale at (a) 500x magnification, (b) 1000x magnification and (c) 3000x magnification. SEM image shows a slightly rough surface with microcrack. Although quartz is expected to the presence in Scale 2 based on EDX analysis, no typical crystal surface can be observed on the surface of Scale 2 indicating most of Scale 2 is a deposition of clay or precipitation of dissolved sand from the oil well. Quartz or sand particles do not easily dissolve, however, dissolve silica in alkaline condition can form silicate solid scale (Arensdorf, Hoster, Mcdougall, & Yuan, 2010; Arensdorf, Kerr, Miner, Incorporated, & Ellis-toddington, 2011; Sazali, Sorbie, & Boak, 2015).

Table 4.2 Composition of Scale 2 solid scale from EDX analysis

Elements	Weight Percent (%)	Mineral Compositions
Si	23.52 ± 0.663	
O	55.77 ± 1.434	
Al	10.65 ± 0.307	
Fe	2.60 ± 0.208	Silica, quartz, aluminium silicate minerals
K	3.84 ± 0.148	
Ca	1.54 ± 0.104	
Mg	1.02 ± 0.208	

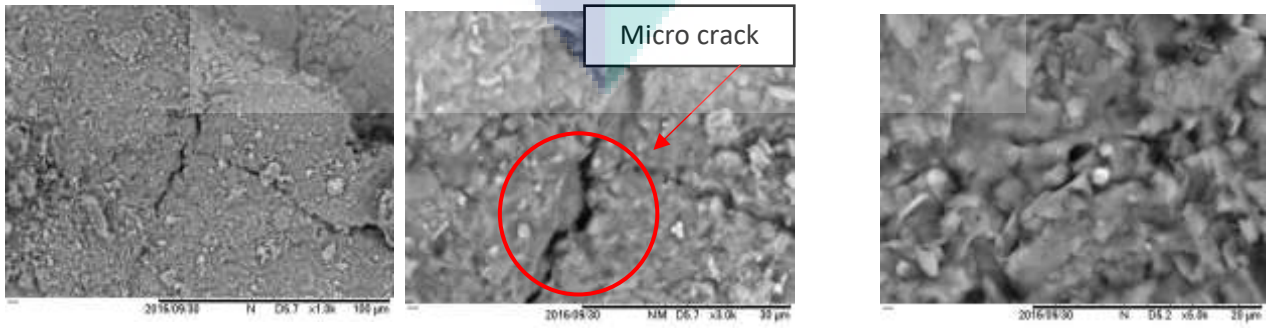

(a) (b) (c)

Figure 4.3 SEM image of Scale 2 solid scale at (a) 500x magnification, (b) 1000x magnification and (c) 3000x magnification.

Table 4.3 show EDX analysis for Scale 3 solid scale to determine possible minerals present in the scale. Based on the EDX analysis, the main elements present are calcium (32.70%), oxygen (50.88%) and carbon (13.92%) with small amount of other metals detected such as iron and magnesium. Based on the element present, it can be concluded that Scale 3 contains mostly of calcite ($CaCO_3$) solid scale. Calcite is one of the most common solid scales that can be found in an oil well. It deposited due to loss of pressure in an oil well with high concentration of calcium ions (Vetter & Farone, 1987). Calcite deposition can occur at a rapid phase compared to another scale (Jasinski et al., 2013; Muryanto et al., 2014) resulting in thick layers of the scale (Figure 4.1). Figure 4.4 shows SEM image of Scale 3 at (a) 500x magnification, (b) 1000x magnification and (c) 3000x magnification. The calcite crystal is in the form of rhombohedral (Aquilano et al., 2016). From the SEM image of Scale 3, it is difficult to determine the exact shape of rhombohedral crystal structure. However, the crystal surface can still be observed with a step or kink shape in some part of the solid scale (Aquilano et al., 2016; Mullin, 2001). The impurities of the solid scale based on the EDX studies probably cause the typical rhombohedral calcite crystal structure cannot be observed. The cleavage split between the crystal structure can be observed at 3000x magnification (Figure 4.4(c)). This cleavage can be a weak point of the solid scale as it will provide space for absorption of chemical in the dissolution process. The image of Scale 3 also shows some degree of porosity. Though calcite scale commonly occurs in oil production, it is easy to remove with the chemical method (M. Mahmoud et al., 2016; Muryanto et al., 2014; Weyl, 1959)

Table 4.3 Composition of Scale 3 solid scale form EDX analysis

Elements	**Weight Percent (%)**	**Minerals Compound**
Ca	32.70 ± 0.362	Calcite, aragonite, gypsum, ferrite
O	50.88 ± 0.538	
C	13.92 ± 0.362	
Fe	1.63 ± 0.170	
Mg	0.72 ± 0.131	
Al	0.16 ± 0.048	

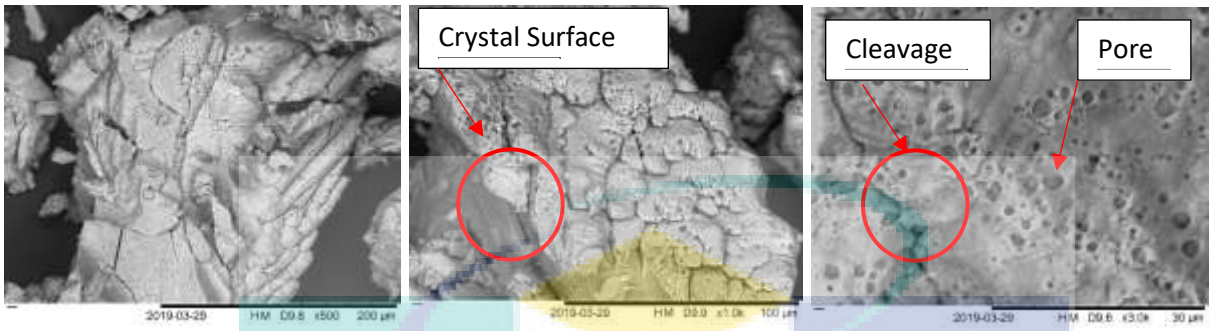

(a) (b) (c)

Figure 4.4 SEM image of Scale 3 solid scale at (a) 500x magnification, (b) 1000x magnification and (c) 3000x magnification.

4.2 Characterisation of Monosodium Glutamate

In this study, a food grade monosodium glutamate (MSG) is used as the main raw material in the synthesis of amino acid based solid scale dissolver. MSG is an organic and non-toxic material often used in food industries. The MSG used in this study come in white crystal form. Figure 4.5 shows the 3D structure of MSG. MSG contains two carboxylic groups (-COOH) and one amine ($-NH_2$) that can bind with metals ion to form a chelate. The melting point of MSG was measured at 227.7 ± 0.36 °C and the density is at 1.7504 ± 0.0188 g/cm^3. The physical properties of MSG were summarised in Table 4.4.

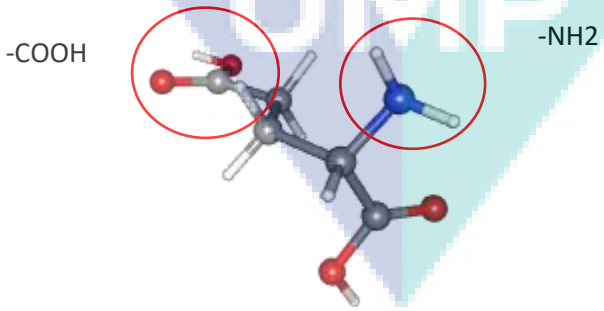

Figure 4.5 Food grade monosodium glutamate crystal used in the synthesis of amino acid based solid scale dissolver.

Table 4.4 Physical properties of food grade monosodium glutamate.

Properties	
Appearance	White crystal, needle-like
Chemical Formula	$C_5H_8NO_4Na$
Melting Point	227.7 ± 0.36 °C
Density	1.7504 ± 0.0188 g/cm3

4.2.1 Infra-red Spectrum of Monosodium Glutamate.

shows the infra-red spectrum of monosodium glutamate (MSG) analysed using Fourier Transform Infra-Red Spectroscopy (FTIR). Monosodium glutamate contains one carboxylic acid group, one carboxylate ion group and one tertiary amine group connected to the carbon chain. Two peaks were observed at a wavelength of 3400 cm-1 and 3630 cm^{-1} indicating the presence of an aliphatic primary amine. Carbonyl (C=O) of carboxylic group bond peak was observed at wavelength 1710 cm^{-1}. The broad peak between 3000 -2500 cm^{-1} indicating the presence of -OH group. The peak at 1380 cm^{-1} indicating the- OH group presence is part of the carboxylic group in the MSG. FTIR spectrum is in agreement with the structure of monosodium glutamate. The presence of -COOH group in MSG is targeted to the presence in the amino acid based solid scale dissolver to bind with the metals ions and form a chelate.

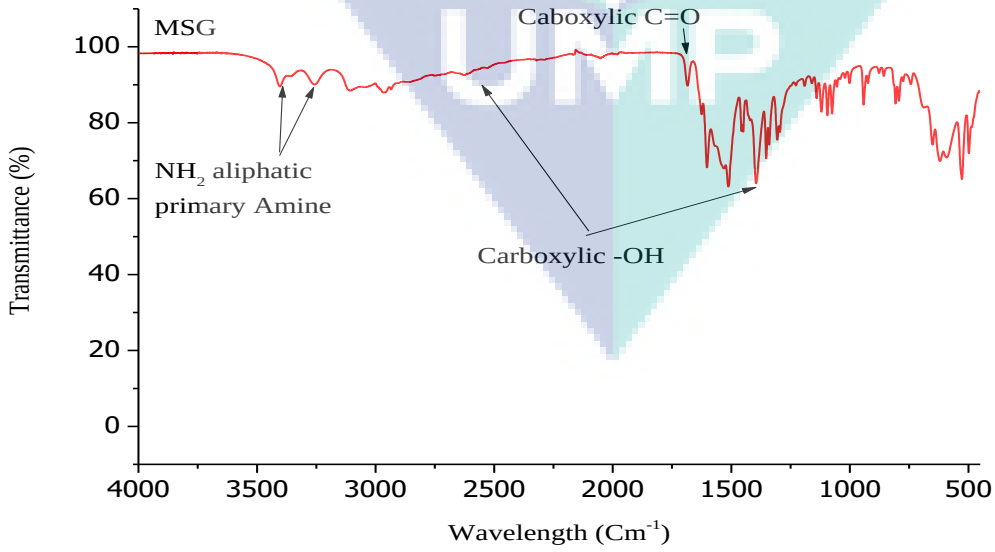

Figure 4.6

shows the infra-red spectrum of monosodium glutamate (MSG) analysed using Fourier Transform Infra-Red Spectroscopy (FTIR). Monosodium glutamate contains one carboxylic acid group, one carboxylate ion group and one tertiary amine group connected to the carbon chain. Two peaks were observed at a wavelength of 3400 cm-1 and 3630 cm^{-1} indicating the presence of an aliphatic primary amine. Carbonyl (C=O) of carboxylic group bond peak was observed at wavelength 1710 cm^{-1}. The broad peak between 3000 -2500 cm^{-1} indicating the presence of -OH group. The peak at 1380 cm^{-1} indicating the- OH group presence is part of the carboxylic group in the MSG. FTIR spectrum is in agreement with the structure of monosodium glutamate. The presence of -COOH group in MSG is targeted to the presence in the amino acid based solid scale dissolver to bind with the metals ions and form a chelate.

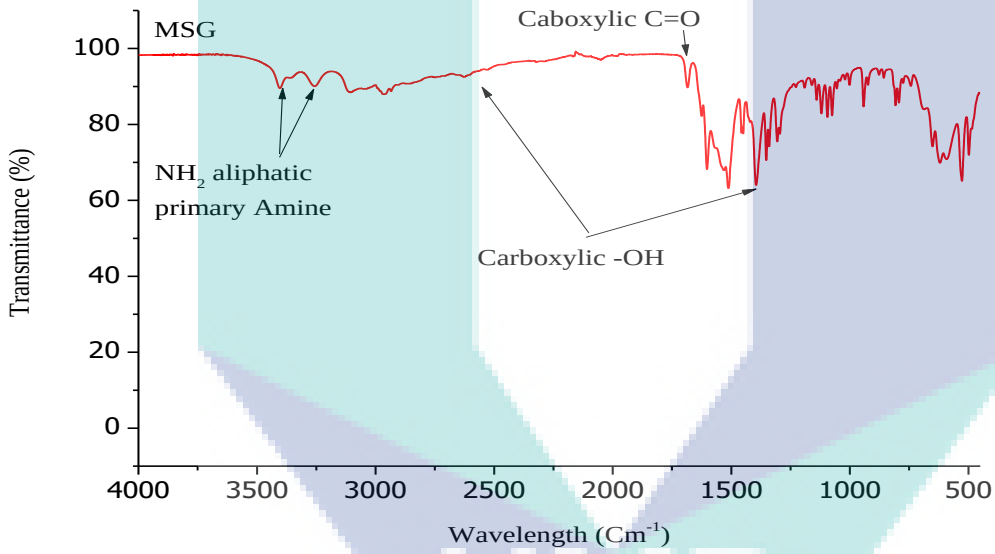

Figure 4.6 Infra-red spectrum of monosodium glutamate

4.2.2 Nuclear Magnetic Resonance Spectroscopy of Monosodium Glutamate.

Monosodium glutamate used in this study was further investigated using nuclear magnetic resonance (NMR) for the detection of carbon (C-NMR). Figure 4.7 Show the structure of MSG. Based on the structure, every carbon in the MSG has a different type of carbon. All carbon type in the MSG was assigned with different labels; a, b, c, and e. Carbon a and e both bonded with two oxygen but have different neighbouring carbon atom. Albeit carbon b and c are both -CH2, there are bonded with different neighbouring carbon and expected to produce a different peak in the C-NMR spectroscopy. Carbon d that bonded to nitrogen is labelled as carbon d.

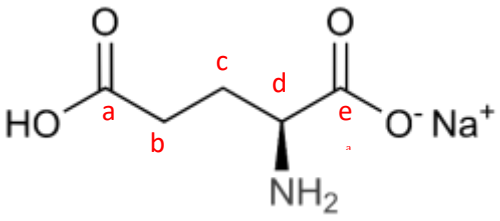

Figure 4.7 Structure of monosodium glutamate with every carbon type is labelled with a, b, c, d and e for recognition purpose.

Figure 4.8 shows the C-NMR spectroscopy of MSG. Five peaks was detected in C-NMR indicating 5 types of carbon detected. Due to the high electronegativity of oxygen, chemical shift for the carboxylic group in C-NMR is between 165-190 ppm. Nitrogen is more electronegative than carbon thus carbon d that connected to nitrogen is expected to affect the chemical shift of carbon c and e. Two peaks were detected in this range at 174.5347 ppm and 181.2739 ppm that can both be assigned for carbon a and e respectively in MSG. The chemical shift of alkane is between 10-50 ppm. In Figure 5.8, two peaks were detected between 10-50 ppm range. Carbon c is mostly shielded from the electronegativity of oxygen. Thus, at peak at 26.9123 ppm is assigned to carbon c while at 33.4158 ppm for carbon b. Peak detected at 54.5755 ppm can be assigned to carbon d. MSG was not analysed for its proton in nuclear magnetic resonance due to the presence of hydroxyl (-OH) and amine group (-NH2). Proton NMR for these groups will appear over a wide range of chemical shift values, having broad signals and have no splitting pattern.

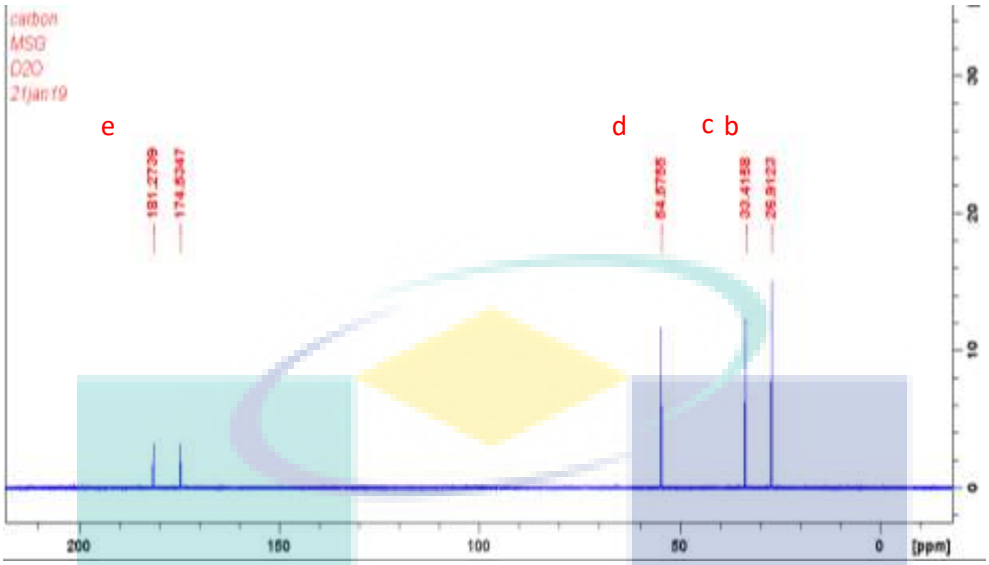

Figure 4.8 Carbon-13 nuclear magnetic Resonance Spectroscopy of Monosodium Glutamate. Label a, b, c, d, and e ware carbon type assigned in MSG (Figure 5.8)

4.2.3 Differential Scanning Calorimetry of Monosodium Glutamate

Figure 4.9 shows the differential scanning calorimetry thermogram of monosodium glutamate crystal. From the DSC thermogram, the endothermic peak was observed at temperature 168.27 ºC, 204.77 ºC and 228.62 ºC. The peak at 168.27 °C can be associated with changes of MSG from its

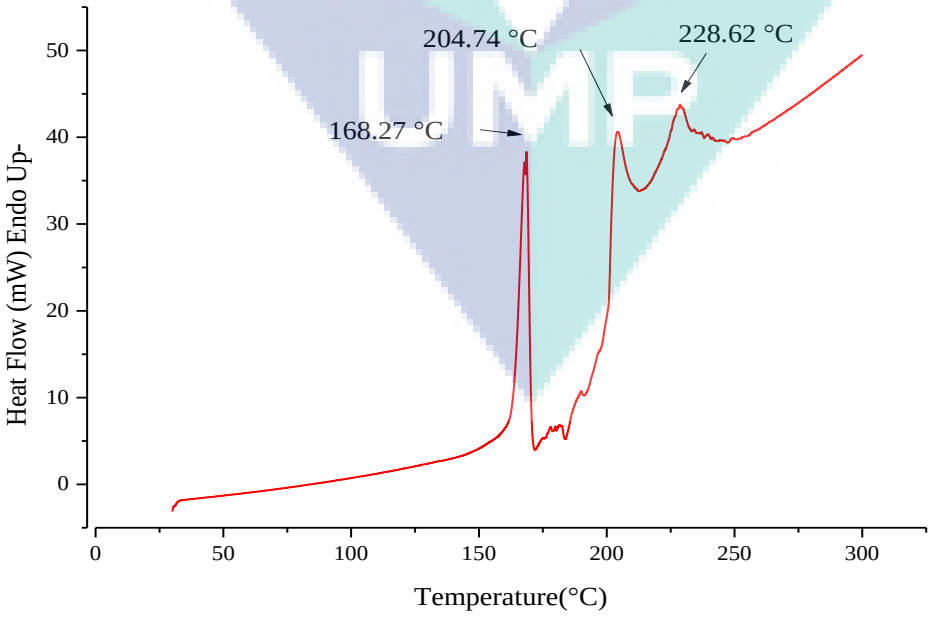

monohydrate to anhydrous form that start to occur at temperature 155 ℃ (Gron et al., 2003). The endothermic peak at 228.62 ^{o}C is corresponding to melting temperature (T*m*) of MSG, in agreement with melting point 227.7 ± 0.36 ℃ measured using melting point analyser as shown in Table 5.4. From literature, melting point (decomposes) of MSG was recorded at 225 ^{o}C (O'Neil, 2001).

Figure 4.9 Differential scanning calorimetry thermogram of monosodium glutamate

4.3 Glutamic Acid from Acidification of Monosodium Glutamate

Acidification of monosodium glutamate (MSG) using hydrochloric acid produces a dwhite compound, L-Glutamic Acid. The mechanism of the reaction is shown in Figure 5.10 where hydrochloric acid will protonate carboxylate ions (-$COO^{-}Na^{+}$) producing L-glutamic acid and sodium chloride (Borissova et al., 2005). The sodium chloride was washed with water. This reaction has 62.09 ±2.34 % yield with sodium chloride by-product. Some of the product of synthesis may be lost during washing using deionised water. CHNS analysis was conducted on the product to determine the percentage of the element present in the product. Theoretically, L-glutamic acid should contain 40.82 % of carbon 43.57 % of oxygen, 9.52 % of nitrogen and 6.12 % hydrogen. CHNS analysis (Table 4.5) shows that L-glutamic acid produce from acidification the elemental percentage is close to theoretical value with 38.54 % carbon, 9.01 % nitrogen, and 6.16 % hydrogen. EDX analysis (Table 4.6) performed on the product shows the percentage of the element present are 45.45 % of carbon, 42.81 % of oxygen, 9.76 % of nitrogen, 0.57 % sodium and 1.46 % of chlorine. This result is close to the theoretical percentage of an element in L-glutamic acid. A small trace of sodium and chloride was detected as impurities (2.03%) in the final product.

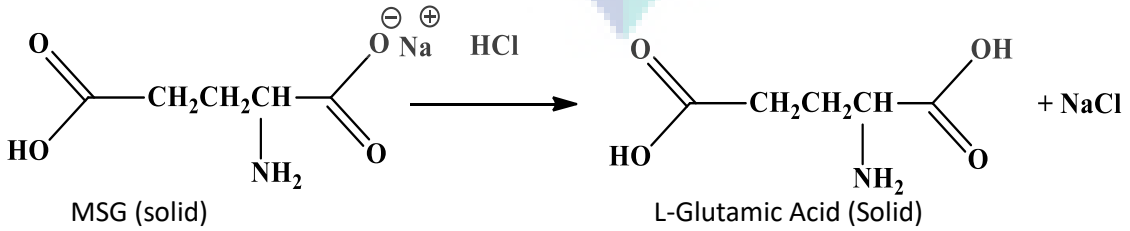

MSG (solid) L-Glutamic Acid (Solid)

Figure 4.10 Reaction mechanism of acidification of monosodium glutamate to produce L-Glutamic acid.

Table 4.5 CHNS analysis of L-glutamic acid produce from acidification of monosodium glutamate.

Element	Theoretical %	CHNS %
Carbon	40.82	38.54
Nitrogen	9.52	9.01
Hydrogen	6.12	6.16
Sulphur	-	0.19

Table 4.6 EDX analysis of L-glutamic acid produced from acidification of monosodium glutamate.

Element	Theoretical %	EDX %
Carbon	40.82	45.45 ± 3.215
Oxygen	43.57	42.81 ± 3.033
Nitrogen	9.52	9.76 ± 5.570
Hydrogen	6.12	Not Measured
Sodium	-	0.57 ± 0.116
Chloride	-	1.46 ± 0.231

Figure 4.11 shows the infra-red spectroscopy of L-glutamic acid produces from the acidification of MSG compared with standard L-glutamic acid purchased from Sigma-Aldrich. Product from precipitation of L-glutamic acid from MSG is comparable with standard L-glutamic acid.

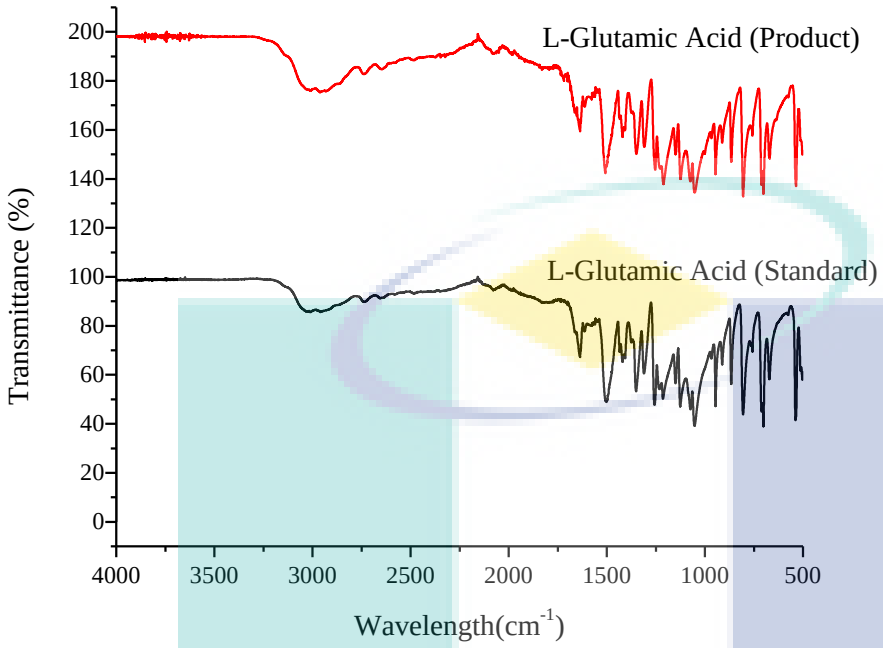

Figure 4.11 FTIR spectroscopy of L-Glutamic acid product from acidification of MSG compared with standard L-Glutamic acid purchased from the Sigma-Aldrich.

4.4 Glutamic Acid Hydrochloride from acidification of L-Glutamic Acid.

4.4.1 Synthesis Mechanism of Glutamic Acid Hydrochloride

L-glutamic acid produce form acidification of monosodium glutamate (Chapter 5.5) was acidified to produce glutamic acid hydrochloride (GluHCl). The reaction mechanism of this reaction is shown in Figure 4.12. In this reaction, hydrochloric acid protonates amine group of L-glutamic acid resulting in amino acid with amine salt. This reaction yields 70.08 ± 1.621% of the product. The separation and yield calculation were explained in the methodology chapter.

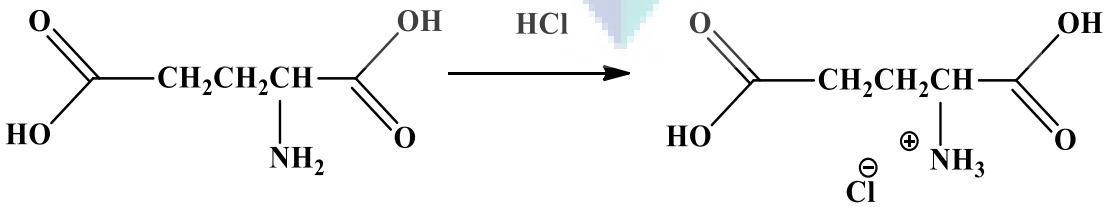

L-Glutamic Acid (Solid) GluCl (Solid, dissolved in water)

Figure 4.12 Synthesis mechanism for the production of glutamic acid hydrochloride form acidification of L-glutamic acid with hydrochloric acid.

4.4.2 Characterisation of Glutamic Acid Hydrochloride

Table 4.7 shows the properties of glutamic acid hydrochloride produce in this study. Glutamic acid hydrochloride (GluCl) is solid at room temperature with melting point 219.68 ± 0.97 °C and completely miscible in water. The density of GluCl is 0.5755 g/cm^3. CHNS analysis of the compound in Table 4.8 shows that it has 29.8% carbon, 9.01 % nitrogen and 6.16 % hydrogen. This value is close to the theoretical value calculated for GluCl with sulphur detected as impurities. EDX analysis results in Table 4.9 shows that the product contains 43.13 % carbon, 39.42 % oxygen, 9.76 % nitrogen and 17.27 % chlorine. This value is close to theoretical value with the exception of carbon that has a higher percentage. The presence of chlorine close to theoretical percentage indicating successful reaction with a small amount of sodium detected as impurities.

Table 4.7 Properties of glutamic acid hydrochloride

	Glutamic Hydrochloride
Yield	70.08 ± 1.621%
Appearance	White Crystalline Powder
Melting point	219.68 ± 0.97 °C
Solubility	Soluble in water
Density	0.5755 ± 0.0087 g/cm3

Table 4.8 CHNS analysis of glutamic acid hydrochloride

Elements	**Theoretical %**	**CHNS %**
Carbon	32.71	29.8
Nitrogen	7.63	9.01
Hydrogen	5.45	6.16
Sulphur	-	0.31

Table 4.9 EDX analysis of glutamic acid hydrochloride

Element	**Theoretical %**	**EDX %**
Carbon	32.71	43.13 ± 0.804

Oxygen	34.89	39.42 ± 0.649
Nitrogen	7.63	9.76 ± 5.570
Chlorine	19.32	17.27 ± 0.286
Sodium		0.18 ± 0.056

Figure 4.13 shows the infra-red spectrum of glutamic acid hydrochloride obtained from this study compares with L-glutamic acid. Both compounds show the peaks for carboxylic -OH bond and amine. However, glutamic hydrochloride has broad aliphatic primary amine at wavelength 3500 cm^{-1} that are not present in L-glutamic acid. In glutamic hydrochloride, amine act as cations consists of three hydrogens attached compare to two in L-glutamic acid. This probably increases the presence of -NH stretch in the infrared spectroscopy. In addition, the peak for amine salt can be observed at wavelength 1600 cm^{-1} in glutamic acid hydrochloride (Heacock & Marion, 1956).

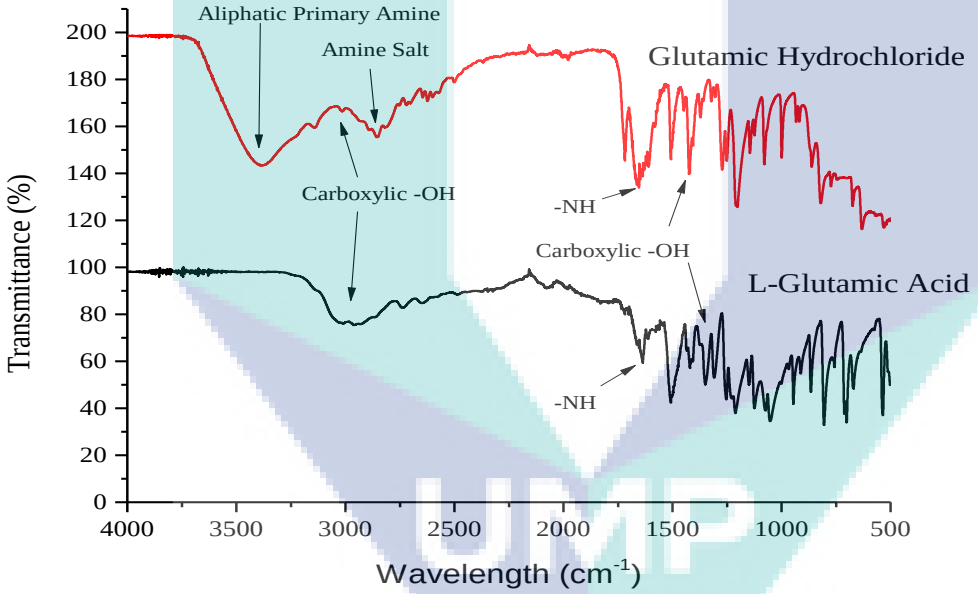

Figure 4.13 FTIR spectroscopy of glutamic hydrochloride compare with L-glutamic acid

Figure 4.14 shows the analysis of glutamic acid hydrochloride using differential scanning calorimetry. The result shows the heat flow peak occurs at a temperature from 178.9 ºC to 229.5 ºC with the highest peak recorded at 208.28 ºC. with ΔH=438.7336 J/g. Based on the melting point monitoring analysis, the melting point is measured at around 219.68 ºC. As there is only one major peak observed in the DSC result, it is likely simultaneous melting and decomposition occur. In

comparison, the previous study measured the melting point of glutamic hydrochloride at 137.2 °C (Rong et al., 2008) much lower compared with the melting point measured in this study.

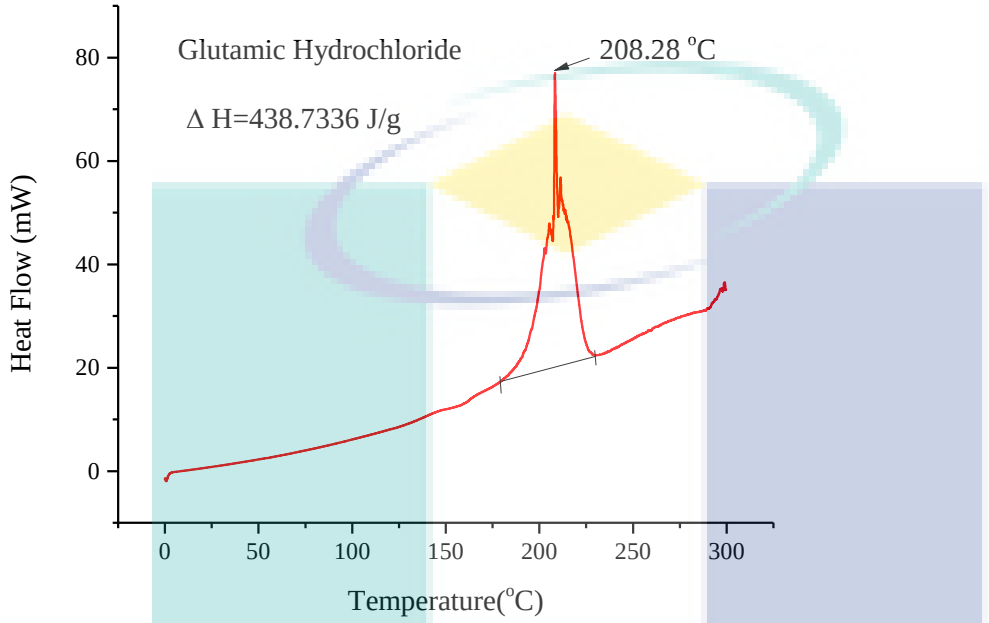

Figure 4.14 Differential Scanning Calorimetry of glutamic hydrochloride

4.4.3 Dissolution of Calcite and Barite in Glutamic Acid Hydrochloride

GluCl produced in this reaction was evaluated for dissolution capability for two types of solid scale; calcium carbonate ($CaCO_3$) and barite ($BaSO_4$). To control the pH, potassium hydroxide (KOH) was used to control the pH of the solution. The amount of KOH used to control the pH for 500 ml of solution is between 5-7 g. Thus, the solubility of both scale in 0.25M of KOH solution was first determined. Table 4.8 shows the concentration of calcium and barite detected in the KOH solution after dissolution for 24 hours at 60 °C. Albeit KOH is used as one of the synergist in barite dissolution (Bageri et al., 2017), the result shows that at concentration of 0.25M, KOH does not dissolve calcite and barite. Thus, the used of KOH for pH control will not significantly affect the dissolution result. GluCl 20g/L solution used in the dissolution have pH value at 1.69. At pH 1.69. The GluCl solution can dissolve up to 3865 ppm of calcium in 24 hours at 60 °C and less than

5ppm of barium. Increasing the pH of the solution to 11.69 reduce the dissolution of calcite to just 14.62 and barite to 3.67 ppm.

Table 4.10 ICP-OES result for the concentration of calcium and barium ions in the solution of 0.25M KOH after dissolution for 24 hours at 60 °C

Solid Scale	Metal Ion Tested	Metals ions Detected (ppm)
CaCO3	Ca^{+2}	Not Detected
BaSO4	Ba^{+2v}	3.26 ± 0.056

Table 4.11 ICP-OES result for concnetration of calcium and barium ion in the solution of GluCl after dissolution for 24 hours at 60 °C

pH	Solid Scale	Metal Ion Tested	Metals ions Detected (ppm)
1.69	CaCO3	Ca^{+2}	3865 ± 21.213
	BaSO4	Ba^{+2}	4.794 ± 0.147
11.69	CaCO3	Ca^{+2}	14.62 ± 0.007
	BaSO4	Ba^{+2}	3.672 ± 0.464

4.5 Glutamic Acid Tetrafluoroborate from Acidification of L-Glutamic Acid.

4.5.1 Synthesis Mechanism of Glutamic Acid Tetrafluoroborate

Glutamic acid tetrafluoroborate produced through acidification of L-Glutamic acid with tetra fluoroboric acid. The reaction scheme is shown in Figure 4.15. In this reaction, hydro fluoroboric acid protonates amine group in L-glutamic acid resulting in amino acid with amine salt. This reaction yields the mixture of approximately 25 ml of thick viscous liquid with white crystallised precipitate at room temperature as shown in Figure 4.16. A further attempt to crystallised or dried the product has not shown any significant result. This property is similar to the previous synthesis by Rong et al. (2008) in which L-glutamic acid tetrafluoroborate (GluBF4) was described as "straw yellow ropy liquid" at room temperature. Such properties indicate that GluBF4 is ionic liquid. The white precipitate only appears once the product was cooled to room temperature after evaporation (rotary evaporator).

Figure 4.15 Synthesis mechanism for the production of glutamic acid tetrafluoroborate form acidification of L-glutamic acid with tetrafluoro boric acid

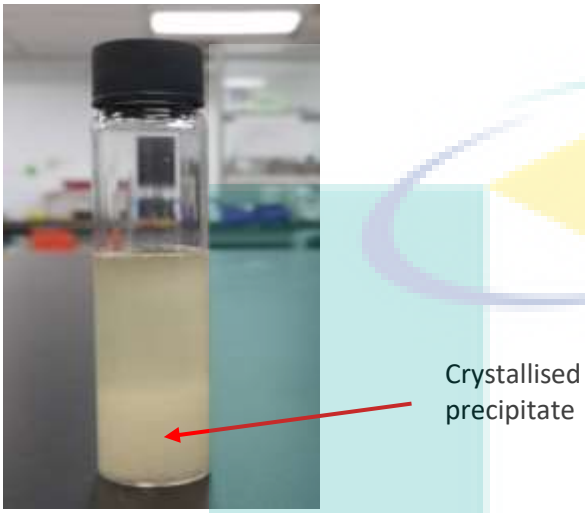

Figure 4.16 FTIR spectroscopy of glutamic acid tetrafluoroborate compare with glutamic acid hydrochloride

4.5.2 Characterisation of Glutamic Acid Tetrafluoroborate

The density of $GluBF_4$ produce was measured at 0.3138 g/cm^3. This density was measured while the $GluBF_4$ was in liquid form. $GluBF_4$ was analysed using FTIR as shown in Figure 4.17. In the acidification process, glutamic acid has one protonation site from amine (Borissova et al., 2005). Acidification of glutamic acid will protonate the amine group becoming amine salt ($-NH_3$) The spectrum shows the peak at 1600 cm^{-1} indicating the presence of amine salt in the product (Heacock & Marion, 1956). The infrared spectrum also shows that acidification does not affect the carboxylic group glutamic acid. The peak of the carboxylic group can be observed at wavelength 3200 cm^{-1} for hydroxyl and 1720 cm-1 for carbonyl.

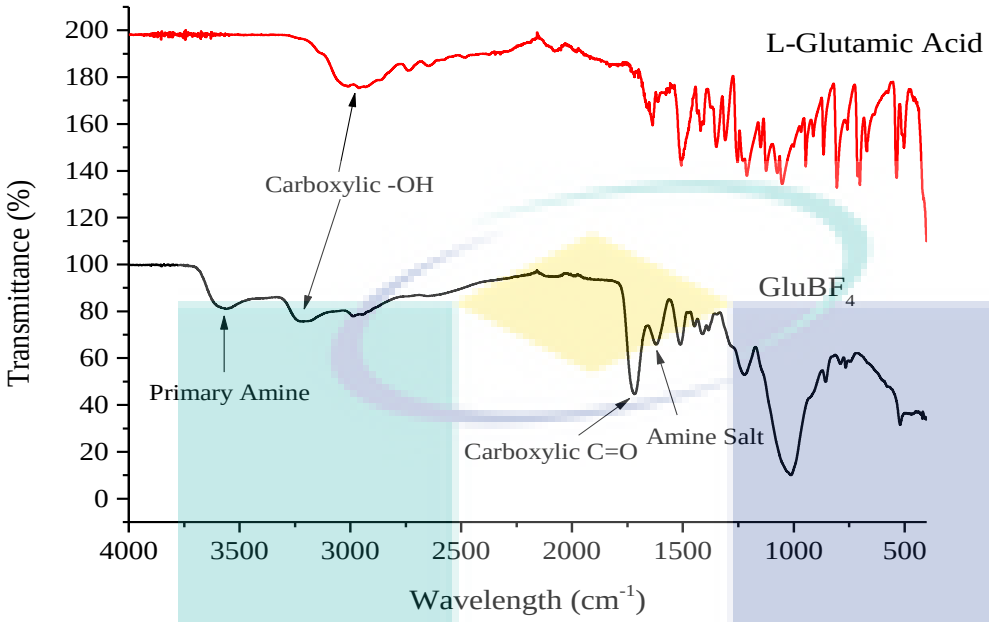

Figure 4.17 FTIR spectroscopy of glutamic acid tetrafluoroborate compare with glutamic acid hydrochloride

CHNS analysis of $GluBF_4$ does not agree with the theoretical value calculated. $GluBF_4$ should have 25.55% carbon, 5.96 % nitrogen and 4.26 % hydrogen. However, CHNS analysis detects 18.69% Carbon, 3.49% nitrogen and 3.312% hydrogen. EDX analysis also gives a different elemental percentage from theoretical value; 23.88% carbon, 19.15 % oxygen, 9.76 % nitrogen, 54.91% fluorine and no boron detected. Though FTIR spectrum indicates the possibility of a successful reaction, CHNS and EDX analysis shows the possibility of incomplete reaction or production of by-product.

Table 4.12 CHNS analysis of glutamic acid tetrafluoroborate

Element	Theoretical %	CHNS Analysis
Carbon	25.55	18.69
Nitrogen	5.96	3.49
Hydrogen	4.26	3.31

Table 4.13 EDX analysis of glutamic acid tetrafluoroborate

Element	Theoretical %	EDX %
Carbon	25.55	23.88 ± 0.417
Oxygen	27.25	19.15 ± 0.649
Nitrogen	5.96	9.76 ± 5.570
Fluorine	32.36	54.91 ± 0.392
Boron	4.59	Not Detected.

4.5.3 Dissolution of Calcite and Barite with $GluBF_4$

$GluBF_4$ produced in this reaction was evaluated for dissolution capability for two types of solid scale; calcium carbonate ($CaCO_3$) and barite ($BaSO_4$). To control the pH, potassium hydroxide (KOH) was used to control the pH of the solution. 20ml/L of $GluBF_4$ in water was prepared and the pH measured is 1.63. The pH of the solution can be increased up to only 5.9-6 as GluBF4 tend to not soluble in water at high pH. Table 4.14 shows the dissolution result of calcite and barite in $GluBF_4$ solution. At a concentration of 20ml/L and pH 1.63. Glu-Bf4 can dissolve up to 2381 ppm of calcium and only 74 ppm of barium. Increasing the pH of the solution to 5.98 decreases the dissolution of the solid scale to only 14.55 ppm of calcium and 65 ppm of barium.

Table 4.14 ICP-OES result for the concentration of calcium and barium ion in the solution of $GluBF_4$ after dissolution for 24 hours at 60 °C

pH	Solid Scale	Metals ion tested	Metals ions Detected (ppm)
1.63	$CaCO_3$	Ca^{+2}	2381 ± 218.58
	$BaSO_4$	Ba^{+2}	74 ± 27.71
5.98	$CaCO_3$	Ca^{+2}	14.550± 0.071
	$BaSO_4$	Ba^{+2}	65 ± 17.04

4.6 Glutamic acid Trifluoromethyl Sulfonate

4.6.1 Synthesis Mechanism of Glutamic Acid Trifluoromethyl Sulfonate

Synthesis of glutamic acid trifluoromethyl sulfonate (GluTFMS) produces yellow viscous liquid at room temperature. The synthesis mechanism is shown in Figure 4.18. In this reaction, the equimolar concentration of GluCl reacts with sodium trifluoromethyl sulfonate (NaTFMS) producing GluTMSF with sodium chloride by-product. This reaction yields 65.92 ± 2.10 % of the product.

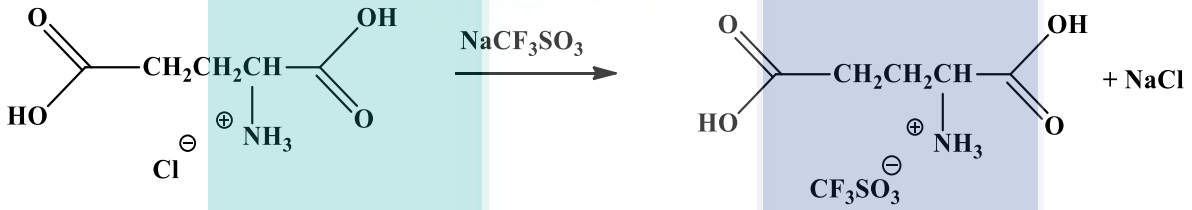

Figure 4.18 Reaction scheme of GluTFMS from metathesis of GluCl with sodium trifluoromethyl sulfonate.

4.6.2 Characterisation of Glutamic Acid Trifluoromethyl Sulfonate

Glutamic acid trifluoromethyl sulfonate (GluTFMS) produce in this study is viscous transparent yellow liquid at room temperature with a density of 1.1774 ± 0.0059 g/cm^3. Base on observation, exposing the liquid to air will slowly cause the viscosity of the liquid to reduce. This indicates the hydrophilic properties of GluTFMS, absorbing the moisture from the air. Figure 4.19 shows the infra-red spectrum of GluTFMS compared with a reactant, GluCl. The infra-red spectrum shows the presence of the sulfonate group in the product at wavelength 1170 cm^{-1} and 1032 cm^{-1} as well as fluoro (C-F) compound. The spectrum shows that the product retains its carboxylic and amine group. This spectrum gives an early indication of a successful reaction in producing GluTFMS form metathesis of GluCl. Analysis using CHNS (Table 4.15) shows that the product contains 19.14 % carbon, 4.01 % hydrogen, 2.92 % nitrogen and 10.06 % of sulphur. Only hydrogen and sulphur have the percentage close to theoretical value while carbon and nitrogen show differences around 5% and 2 % respectively.

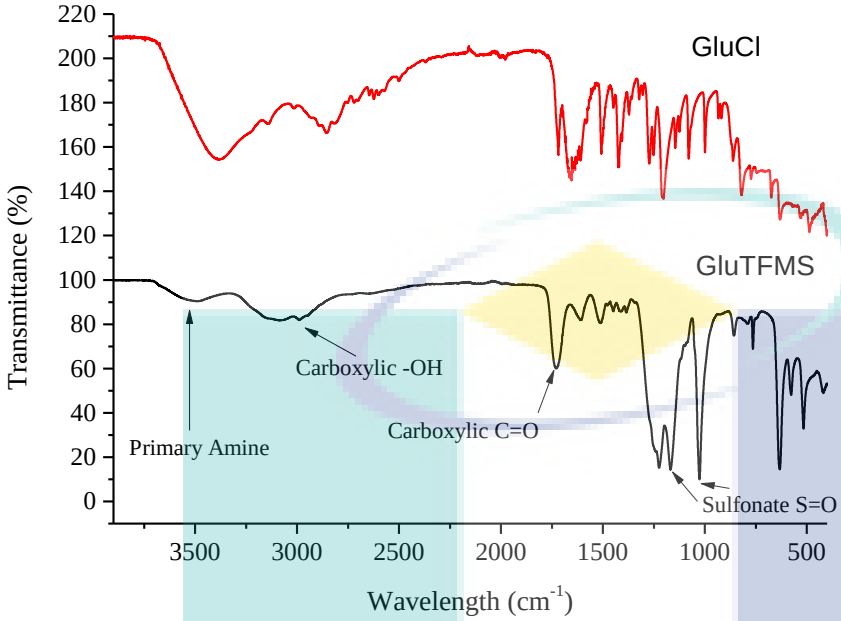

Figure 4.19 Infra-red spectrum of GluTFMS produce from metathesis of GluCl with sodium trifluoromethyl sulfonate

Table 4.15 CHNS analysis of GluTFMS

Element	Theoretical %	CHNS %
C	24.24242	19.14
H	3.367003	4.01
N	4.713805	2.92
S	10.77441	10.06

4.6.3 Dissolution of Calcite and Barite with GluTFMS

GluTFMS produced in this reaction was evaluated for dissolution capability for two types of solid scale; calcium carbonate ($CaCO_3$) and barite ($BaSO_4$). Due to the limited amount of GluTFMS produced, the dissolution was only done at pH of the prepared solution. 10ml/L of GluTFMS solution was prepared and the pH recorded at 2.50. Table 4.16 shows the dissolution result of calcite and barite in GluTFMS solution. At a concentration of 10 ml/L, pH 2.5, for 24 hours at 60

°C, GluTFMS can dissolve up to 2013.5 ppm of calcium and 60.0 ppm of barite. Considering the aqueous solution of GluTFMS is used, this dissolution result considered good.

Table 4.16 ICP-OES result for the concentration of calcium and barium ion in the solution of GluTFMS after dissolution for 24 hours at 60 °C

pH	Solid Scale	Metals ions Detected (ppm)
2.5	$CaCO_3$	2013.5 ± 65.76
	$BaSO_4$	60.0 ± 7.07

CHAPTER 5

CONCLUSION

5.1 Conclusion

The aim of this study is to simulate the molecular dynamic of the chelate agent glutamic acid diacetic acid (GLDA) and glutamic acid diacetic acid tetrasodium salt (GLDA-Na_4), to synthesis the amino acid based solid scale dissolver and to evaluate the dissolution capability of the dissolver for calcite and barite. The key finding of this study are:

i) Three solid scales obtained from oil well has been analysed to understand the composition and surface morphology of the real solid scale. Solid Scale 1 is determined as barite that has a yellowish or light brown colour contains 43.12 % barium, 30.86 % oxygen, 9.57 %sulphur, carbon 14.42 % and 1.37% strontium with other trace element. The minerals present in Scale 1 is barium sulphate ($BaSO_4$), barium oxide (BaO) and strontium oxide (SrO). Scale 1 has crystalline surface; steps, kink, and edge vacancies indicates the barite crystal growth slowly over time and forming a layer of scale. Solid Scale 2 is determined as silicate scale with 55.77 % of oxygen and 23.52 % of silicon. SEM image shows no characteristic of crystalline surface. Based on this Scale 2 is a deposition of mud and fine sand from the production well. Solid Scale 3 is determined as calcite with 32.70% of calcium, 50.88% of oxygen and 13.92% of carbon. The presence of carbon come from hydrocarbon material that coat the surface of the scale.

ii) This study has synthesis three amino acid based solid scale dissolver; glutamic acid hydrochloride (GluCl), glutamic acid tetrafluoroborate ($GluBF_4$) and glutamic acid

trifluoromethyl sulfonate and (GluTFMS). Glutamic acid hydrochloride is white solid at room temperate with melting point at 219.68 °C and have a density of 0.5755 g/cm^3. $GluBF_4$ is thick viscous yellowish liquid with white crystallised precipitate at room temperature with density of 0.3138 g/cm^3. GluTFMS is thick viscous yellowish liquid at room temperature with density of 1.1774 g/cm^3. All of this dissolver was soluble in water.

iii) The dissolution capability of the solid scale dissolver was determine using dissolution test. GluCl 20g/L solution used in the dissolution have pH value at 1.69 and 11.69. At pH 1.69 The GluCl solution can dissolve up to 3865 ppm of calcium in 24 hours at 60 °C and less than 5ppm of barium. Increasing the pH of the solution to 11.69 reduce the dissolution of calcite to just 14.62 and barite to 3.67 ppm. For $GluBF_4$, the dissolution was conducted at pH 1.63 and 5.98. $GluBF_4$ was not dissolve at pH higher than 6. At a concentration of 20ml/L and pH 1.63, Glu-BF_4 can dissolve up to 2381 ppm of calcium and only 74 ppm of barium. Increasing the pH of the solution to 5.98 decreases the dissolution of the solid scale to only 14.55 ppm of calcium and 65 ppm of barium. Due to the limited amount of GluTFMS produced, the dissolution was only done at pH of the prepared solution (pH 2.50). At 10ml/L of concentration, pH 2.5, for 24 hours at 60 °C, GluTFMS can dissolve up to 2013.5 ppm of calcium and 60.0 ppm of barite. Based on the dissolution result, GluCl, GluBF4 and Glu TFMS is a good dissolver for calcite as it can dissolve more than 2000 ppm of calcite at low concentration. Barite is known as the most difficult solid scale to dissolve. In this study, all three dissolver synthesised can only dissolve less than 100 ppm of barite.

REFERENCES

Abass, H. H., Nasr-El-Din, H. A., & BaTaweel, M. H. (2002). Sand Control: Sand Characterization, Failure Mechanisms, and Completion Methods. Proceedings - SPE Annual Technical Conference and Exhibition, 2997-3004.

Aquilano, D., Otálora, F., Pastero, L., & García-Ruiz, J. M. (2016). Three study cases of growth morphology in minerals: Halite, calcite and gypsum. Progress in Crystal Growth and Characterization of Materials, 62 (2), 227-251.

Arensdorf, J., Hoster, D., McDougall, D., & Yuan, M. (2010). Static and Dynamic Testing of Silicate Scale Inhibitors. Paper presented at the International Oil and Gas Conference and Exhibition in China, 8-10 June, Beijing.

Bageri, B. S., Mahmoud, M. A., Shawabkeh, R. A., Al-Mutairi, S. H., & Abdulraheem, A. (2017). Toward a Complete Removal of Barite (Barium Sulfate $BaSO_4$) Scale Using Chelating Agents and Catalysts. Arabian Journal for Science and Engineering, 42 (4), 1667-1674.

Basbar, A. E. A., Elraies, K. A., & Osgouei, R. E. (2013). Formation Silicate Scale Inhibition during Alkaline Flooding: Static Model. Paper presented at the North Africa Technical Conference and Exhibition, 15–17 April Cairo, Egypt.

Bhaduri, S., Shen, D., & Gupta, D. V. S. (2018). Application of Solid Scale Inhibitor in Annular Space to Reduce Well Intervention Cost. Paper presented at the SPE International Conference and Exhibition on Formation Damage Control.

Borissova, A., Jammoal, Y., Javed, K. H., Lai, X., Mahmud, T., Penchev, R., Roberts, K. J., & Wood, W. (2005). Modeling the Precipitation ofl-Glutamic Acid via Acidification of Monosodium Glutamate. Crystal Growth & Design, 5 (3), 845-854.

Brennecke, J. F., & Maginn, E. J. (2004). Ionic liquids: Innovative fluids for chemical processing. AIChE Journal, 447 (11), 2384-2389.

Brown, M. (1998). "Full Scale Attack" Review. *The BP Technology Magazine*, 30-32.

Chen, T., Wang, Q., Chang, F. F., & Al-Janabi, Y. T. (2016). New Developments in Iron Sulfide Scale Dissolvers. In: NACE International.

Crabtree, M., Eslinger, D., Fletcher, P., Miller, M., Johnson, A., & King, G. (1999). Fighting Scale — Removal and Prevention. Oilfield Review, 11 (3), 30-45.

Di Lullo, G., & Rae, P. (1996). A New Acid for True Stimulation of Sandstone Reservoirs. Paper presented at the SPE Asia Pacific Oil and Gas Conference, 28-31 October, Adelaide, Australia.

Dunn, K., & Yen, T. F. (1999). Dissolution of Barium Sulfate Scale Deposits by Chelating Agents. Environmental Science & Technology, 33 (16), 2821-2824.

Economides, M. J. (2012). Petroleum Production Systems: Pearson Education, Limited.

Ezekwe, N. U. h. b. g. c. m. b. i. T. C. (2010). Petroleum Reservoir Engineering Practice: Pearson Education.

Frenier, W. W., Rainey, M., Wilson, D., Crump, D., & Jones, L. (2013). A Biodegradable Chelating Agent is Developed for Stimulation of Oil and Gas Formations. Paper presented at the SPE/EPA/DOE Exploration and Production Environmental Conference, 2003, San Antonio, Texas, U.S.A.

Frenier, W. W., Wilson, D., Crump, D., & Jones, L. (2000). Use of Highly Acid-Soluble Chelating Agents in Well Stimulation Services. Paper presented at the SPE Annual Technical Conference and Exhibition, 1-4 October, Dallas, Texas.
Fukumoto, K., Yoshizawa, M., & Ohno, H. (2005). Room temperature ionic liquids from 20 natural amino acids. Journal of the American Chemical Society, 127 (8), 2398-2399.
Gao, Y., Arritt, S. W., Twamley, B., & Shreeve, J. n. M. (2005). Guanidinium-based ionic liquids. Inorganic Chemistry, 44 (6), 1704-1712.
Ghalambor, A., & Economides, M. J. (2002). Formation damage abatement: A quarter-century perspective. SPE Journal, 7 (1), 4-13.
Gron, H., Mougin, P., Thomas, A., White, G., Wilkinson, D., Hammond, R. B., Lai, X. J., & Roberts, K. J. (2003). Dynamic in-process examination of particle size and crystallographic form under defined conditions of reactant supersaturation as associated with the batch crystallization of monosodium glutamate from aqueous solution. Industrial & Engineering Chemistry Research, 42 (20), 4888-4898.
Gupta, O. D., Armstrong, P. D., & Shreeve, J. n. M. (2003). Quaternary trialkyl(polyfluoroalkyl)ammonium salts including liquid iodides. Tetrahedron Letters, 44 (52), 9367-9370.
Heacock, R. A., & Marion, L. (1956). The Infrared Spectra of Secondary Amines and Their Salts. Canadian Journal of Chemistry, 34 (12), 1782-1795.
Houseworth, J. (2013). Advanced Well Stimulation Technologies. T.Ccst.Us, 47-88.
Jasinski, R., Fletcher, P., Taylor, K., & Sablerolle, W. (2013). Calcite Scaling Tendencies for North Sea HTHP Wells: Prediction, Authentication and Application. Paper presented at the SPE Annual Technical Conference and Exhibition.
Jordan, M. M., Sjuraether, K., Collins, I. R., Feasey, N. D., & Emmons, D. (2001). Life Cycle Management of Scale Control within Subsea Fields and its Impact on Flow Assurance, Gulf of Mexico and the North Sea Basin. In: Society of Petroleum Engineers.
Kelland, M. A. (2014). Production Chemicals for the Oil and Gas Industry, Second Edition (2nd ed.). Boca Raton, Florida: CRC Press.
Lepage, J. N., De Wolf, C. A., Bemelaar, J. H., & Nasr-El-Din, H. A. (2011). An Environmentally Friendly Stimulation Fluid for High-Temperature Applications. SPE Journal, 16 (1), 104-110.
Mackay, E. J. (2007). Oilfield Scale : A New Integrated Approach to Tackle and Old Foe. In (pp. 47-47).
Mahmoud, M., Abdelgawad, K. Z., Elkatatny, S. M., Akram, A., & Stanitzek, T. (2016). Stimulation of Seawater Injectors by GLDA (Glutamic-Di Acetic Acid). SPE Drilling & Completion, 31 (3), 178-187.
Mahmoud, M. A., Nasr-El-Din, H. A., De Wolf, C. A., LePage, J. N., & Bemelaar, J. H. (2011). Evaluation of a New Environmentally Friendly Chelating Agent for High-Temperature Applications. SPE Journal, 16 (3), 559-574.
McSween, H. Y., Richardson, S. M., & Uhle, M. (2004). Geochemistry: Pathways and Processes: Columbia University Press.
Means, J. L., Crerar, D. a., & Duguid, J. O. (1978). Migration of Radioactive Wastes: Radionuclide Mobilization by Complexing Agents. Science, 200 (10), 1477-1481.
Merdhah, A. B. (2007). The Study of Scale Formation in Oil Reservoir During Water Injection at High-barium and High-salinity Formation Water. Master of Engineering (Petroleum), Universiti Teknologi Malaysia, Skudai.

Merdhah, A. B., & Mohd Yassin, A. A. (2009). Scale Formation Due to Water Injection in Malaysian Sandstone Cores. American Journal of Applied Sciences, 6 (8), 1531-1538.
Merdhah, A. B., & Yassin, A. A. (2007). Barium Sulfate Scale Formation in Oil Reservoir During Water Injection at High-Barium Formation Water. Journal of Applied Sciences, 7 (17), 2393-2403.
Moghadasi, J., Müller-Steinhagen, H., Jamialahmadi, M., & Sharif, A. (2007). Scale Deposits in Porous Media and Their Removal By Edta Injection. Heat Exchanger Fouling and Cleaning VII, 59-60.
Mullin, J. W. (2001). Crystallization (4th ed.). Oxford: Butterworth-Heinenmann.
Muryanto, S., Bayuseno, A. P., Ma'mun, H., & Usamah, M. (2014). Calcium Carbonate Scale Formation in Pipes: Effect of Flow Rates, Temperature, and Malic Acid as Additives on the Mass and Morphology of the Scale. Procedia Chemistry, 9, 69-76.
Mutnovskoe, T. H. E., & Field, H. (2000). Study of the Amorphous Silica Scales Formation At The Mutnovskoe Hydrothermal Field (Russia). Proceeding of the Twenty-Fifth Workshop on Geothermal Reservoir Engineering, 24-26 January, Stanford, California.
Nasr-El-Din, H. A., & Al-Humaidan, A. Y. (2001). Iron Sulfide Scale: Formation, Removal and Prevention. Paper presented at the SPE International Symposium on Oilfield Scale 30-31 January, Aberdeen, United Kingdom.
Nassivera, M., & Essel, A. (1979). Fateh Field Sea Water Injection - Water Treatment, Corrosion, And Scale Control. Proceeding of the Middle East Technical Conference and Exhibition, 1979, Bahrain.
O'Neil, M. J. (2001). The Merck index : an encyclopedia of chemicals, drugs, and biologicals (13th ed. ed.). Whitehouse Station, N.J.: Merck.
Olajire, A. A. (2015). A review of oilfield scale management technology for oil and gas production. Journal of Petroleum Science and Engineering, 135, 723-737.
Portier, S., Vuataz, F., Nami, P., Sanjuan, B., & Gerard, A. (2009). Chemical stimulation techniques for geothermalwells: experiments on the three-well EGS system at Soultz-sous-Forêts, France. Geothermics, 38, 349-359.
Rajeev, P., Surendranathan, A. O., & Murthy, C. S. N. (2012). Corrosion mitigation of the oil well steels using organic inhibitors-A review. Journal of Materials and Environmental Science, 3 (5), 856-869.
Ramstad, K., Tydal, T., Askvik, K. M., & Fotland, P. (2005). Predicting carbonate scale in oil producers from high-temperature reservoirs. SPE Journal, 10 (4), 363-373.
Read, P. A., & Ringen, J. K. (1982). The Use of Laboratory Tests to Evaluate Scaling Problems During Water Injection. Society of Petroleum Engineers (SPE-10593), 7-18.
Rong, H., Li, W., Chen, Z., & Wu, X. (2008). Glutamic Acid Cation Based Ionic Liquids : Microwave Synthesis , Characterization , and Theoretical Study. 1451-1455.
Sillanpaa, M., & Oikari, A. (1996). Assessing the Impact of Complextion by EDTA and DTPA on Heavy Metal Toxicity Using Mocrotox Bioassay. Chemosphere, 32 (8), 1485-1497.
Smith, C. F., & Hendrickson, A. R. (1965). Hydrofluoric Acid Stimulation of Sandstone Reservoirs. Journal of Petroleum Technology, 17 (02), 215-222.
Tao, G.-h., He, L., Sun, N., & Kou, Y. (2005). New generation ionic liquids: cations derived from amino acids. Chemical communications (Cambridge, England) (28), 3562-3564.
Terry, R. E., & Rogers, J. B. (2014). Applied Petroleum Reservoir Engineering (3 ed.): Pearson Education.

Tjomsland, T., Grotle, M. N., & Vikane, O. (2013). Scale Control Strategy and Economical Consequences of Scale at Veslefrikk. Paper presented at the International Symposium on Oilfield Scale, 30-31 January, Aberdeen, United Kingdom.
Vetter, O. J. (1975). How Barium Sulfate Is Formed: An Interpretation. Journal of Petroleum Technology, 27 (12), 1515-1524.
Vetter, O. J., & Farone, W. A. (1987). Calcium Carbonate Scale in Oilfield Operations. Paper presented at the SPE Annual Technical Conference and Exhibition, 1987, Dallas, Texas.
Vetter, O. J., Kandarpa, V., & Harouaka, A. (1982). Prediction of Scale Problems Due to Injection of Incompatible Waters. Journal of Petroleum Technology, 34 (02).
Weyl, P. K. (1959). The change in solubility of calcium carbonate with temperature and carbon dioxide content. Geochimica et Cosmochimica Acta, 17 (3), 214-225.
Wigg, H., & Fletcher, M. Establishing the True Cost of Downhole Scale Control, 1995, Aberdeen.
Xue, H., Verma, R., & Shreeve, J. n. M. (2006). Review of ionic liquids with fluorine-containing anions. Journal of Fluorine Chemistry, 127 (2), 159-176.
Zhang, F., Dai, Z., Zhang, Z., Al-Saiari, H., Yan, F., Bhandari, N., Ruan, G., Liu, Y., Lu, Y.-T., Deng, G., Kan, A. T., & Tomson, M. B. (2017). Scaling Risk and Inhibition Prediction of Carbonate Scale at High Temperature. Paper presented at the SPE International Conference on Oilfield Chemistry.
Zhang, P., Kan, A. T., & Tomson, M. B. (2015). Oil Field Mineral Scale Control. In Z. Amjad & K. D. Demadis (Eds.), *Mineral Scales and Deposits* (pp. 603-617). Amsterdam: Elsevier.